Check for updates

ADVANCING EARTH AND SPACE SCIENCE

JGR Atmospheres

RESEARCH ARTICLE
10.1029/2020JD033145

Key Points:
- Ambient hydroxyl group mass correlated strongly to sodium, and their ratio for the limited samples available correlated to dissolved organic carbon normalized by salinity for generated sea spray aerosol
- Non-combustion, likely secondary biogenic, sources contribute 47–88% of submicron organic mass and 21–86% of submicron sulfate during marine periods
- The fraction of particles in the 0.1–0.2 μm size range that were cloud condensation nuclei was highest during early spring due to a larger fraction of hygroscopic sulfate

Supporting Information:
- Supporting Information S1

Correspondence to:
L. M. Russell,
lmrussell@ucsd.edu

Citation:
Saliba, G., Chen, C.-L., Lewis, S., Russell, L. M., Quinn, P. K., Bates, T. S., et al. (2020). Seasonal differences and variability of concentrations, chemical composition, and cloud condensation nuclei of marine aerosol over the North Atlantic. *Journal of Geophysical Research: Atmospheres*, *125*, e2020JD033145. https://doi.org/10.1029/2020JD033145

Received 22 MAY 2020
Accepted 28 AUG 2020
Accepted article online 1 SEP 2020

Author Contributions:
Conceptualization: Lynn M. Russell, Patricia K. Quinn, Timothy S. Bates, Eric S. Saltzman, Craig A. Carlson, Michael J. Behrenfeld
Formal analysis: Georges Saliba, Chia-Li Chen, Savannah Lewis, Lynn M. Russell, Patricia K. Quinn, Timothy S. Bates, Thomas G. Bell, Michael J. Lawler, Kevin J. Sanchez, Richard Moore, Michael Shook, Laura-Helena Rivellini, Alex Lee, Nicholas Baetge, Craig A. Carlson
(continued)

©2020. American Geophysical Union. All Rights Reserved.

Seasonal Differences and Variability of Concentrations, Chemical Composition, and Cloud Condensation Nuclei of Marine Aerosol Over the North Atlantic

Georges Saliba[1], Chia-Li Chen[1], Savannah Lewis[1], Lynn M. Russell[1], Patricia K. Quinn[2], Timothy S. Bates[3], Thomas G. Bell[4,5], Michael J. Lawler[5], Eric S. Saltzman[5], Kevin J. Sanchez[6,7], Richard Moore[6], Michael Shook[6], Laura-Helena Rivellini[8], Alex Lee[8,9], Nicholas Baetge[10], Craig A. Carlson[10], and Michael J. Behrenfeld[11]

[1]Scripps Institution of Oceanography, University of California, San Diego, La Jolla, CA, USA, [2]Pacific Marine Environmental Laboratory, National Oceanic and Atmospheric Administration, Seattle, WA, USA, [3]Joint Institute for the Study of the Atmosphere and Ocean, University of Washington, Seattle, WA, USA, [4]Plymouth Marine Laboratory, Plymouth, UK, [5]Department of Earth System Science, University of California, Irvine, CA, USA, [6]NASA Langley Research Center, Hampton, VA, USA, [7]Universities Space Research Association, Columbia, MD, USA, [8]Environmental Research Institute, National University of Singapore, Singapore, [9]Department of Civil and Environmental Engineering, National University of Singapore, Singapore, [10]Department of Ecology, Evolution and Marine Biology, University of California, Santa Barbara, CA, USA, [11]Department of Botany and Plant Pathology, Oregon State University, Corvallis, OR, USA

Abstract The majority of the aerosol particle number (condensation nuclei or CN) in the marine boundary layer (MBL) consists of sulfate and organic compounds that have been shown to provide a large fraction of the cloud condensation nuclei (CCN). Here we use submicron non-refractory Aerosol Mass Spectrometer (AMS) and filter measurements of organic and sulfate components of aerosol particles measured during four North Atlantic Aerosol and Marine Ecosystems Study (NAAMES) research cruises to assess the sources and contributions of submicron organic and sulfate components for CCN concentrations in the MBL during four different seasons. Submicron hydroxyl group organic mass (OM) correlated strongly to sodium concentrations during clean marine periods ($R = 0.9$), indicating that hydroxyl group OM can serve as a proxy for sea-spray OM in ambient measurements. Sea-spray OM contributed 45% of the sum of sea-spray OM and sea salt during late spring (biomass climax phase) compared to <20% for other seasons, but the seasonal difference was not statistically significant. The contribution of non-combustion sources during clean marine periods to submicron OM was 47 to 88% and to non-sea-salt sulfate 31 to 86%, with likely sources being marine and biogenic. The remaining submicron OM and sulfate were likely associated with ship or continental sources, including biomass burning, even during clean marine periods. The seasonal contribution from secondary sulfate and OM components to submicron aerosol mass was highest during late spring (60%), when biogenic emissions are expected to be highest, and lowest during winter (18%). Removing submicron sea-spray OM decreased CCN concentrations by <10% because of competing effects from increased hygroscopicity and decreased particle size. During all seasons, adding biogenic secondary sulfate increased hygroscopicity, particle size, and CCN concentrations at 0.1–0.3% supersaturations by 5–66%. The largest change was during early spring when the fraction of hygroscopic sulfate components in the 0.1–0.2 μm size range was highest (80%). During continental periods, the increased contribution from low-hygroscopicity organic components to 0.1–0.2 μm diameter particles reduces the CCN/CN by 20–100% for three seasons despite the increased CN and mass concentrations. These results illustrate the important role of the chemical composition of particles with diameters 0.1–0.2 μm for controlling CCN in the MBL.

1. Introduction

Sea-spray aerosol contributes substantial aerosol mass to the marine boundary layer (MBL) (Lewis & Schwartz, 2004) and controls direct radiative forcing over the open ocean (Murphy et al., 1998). Sulfate- and organic-containing particles are ubiquitous in the MBL, providing the largest contributions to the nucleation (particles <0.08 μm dry diameter) and accumulation (particles between 0.08 and 2 μm dry

Funding acquisition: Lynn M. Russell, Patricia K. Quinn, Timothy S. Bates, Michael J. Behrenfeld
Methodology: Georges Saliba, Chia-Li Chen, Lynn M. Russell
Supervision: Lynn M. Russell
Validation: Georges Saliba
Writing - original draft: Georges Saliba, Lynn M. Russell
Writing – review & editing: Georges Saliba, Chia-Li Chen, Savannah Lewis, Lynn M. Russell, Patricia K. Quinn, Timothy S. Bates, Thomas G. Bell, Michael J. Lawler, Eric S. Saltzman, Kevin J. Sanchez, Richard Moore, Michael Shook, Laura-Helena Rivellini, Alex Lee, Nicholas Baetge, Craig A. Carlson, Michael J. Behrenfeld

diameter) modes of the marine number size distribution (Seinfeld & Pandis, 2006). These particles are often the major source of cloud condensation nuclei (CCN) in the MBL, where the contributions from different sources depend on coastal influences (Modini et al., 2015), latitude (Quinn et al., 2017), season (Sanchez et al., 2018), and sea surface temperature (Saliba et al., 2019). However, the magnitudes of contributions from different sources have yet to be completely characterized (see supporting information Text S1 and Table S1). The chemical composition of submicron aerosol particles is important in regions where the cloud droplet concentrations and size are sensitive to CCN concentrations, such as the North Atlantic (Falkowski et al., 1992; Martin et al., 1994; Sorooshian et al., 2020; Yang et al., 2012). To assess the sources of these CCN, we need to evaluate the budget of the main chemical components that contribute to CCN-sized particles—namely, sea salt, organics, and sulfate.

The source of submicron and supermicron sea-spray particles is clearly breaking waves, and a large fraction of the sea-spray particle mass is NaCl and associated sea salts. The amount of organic components that contribute to these submicron particles has been reported to vary from less than 20% to more than 90%. Based on measurements of ambient aerosol, Ovadnevaite, O'Dowd, et al. (2011) reported that up to 97% of the submicron non-refractory organic mass (NR-Org) sampled at Mace Head was marine and likely sea spray during organic sea-spray plumes. Similar conclusions were reached by Ceburnis et al. (2011) at Mace Head for submicron organic carbon during marine periods (defined using surface wind from the North Atlantic ocean, particle number concentrations <700 cm^{-3}, and black carbon concentrations <50 ng/m^3). Miyazaki et al. (2011) used carbon isotopic ratios to identify marine biogenic carbon and found it accounted for 88% of aerosol carbon in the Western North Pacific. Fu et al. (2011) attributed only 33% of the total (submicron and supermicron) organic mass to natural marine sources in the North Atlantic. Virkkula et al. (2006) found evidence of anthropogenic <3 μm diameter organic particle sources in the Atlantic. Huang et al. (2018) found that long-range transport contributed on average 49% of submicron non-refractory organic mass in the eastern Atlantic between 53°N and 53°S. Saliba et al. (2019) found 10–20% seasonal differences in sea-spray organic mass in the North Atlantic for submicron marine periods, assuming that 20% of sea-spray mass is organic as was found for the Western Atlantic. Cachier et al. (1986) reported that more than 80% of submicron carbon was of continental origin from several marine locations in the northern hemisphere. Shank et al. (2012) reported strong correlations between non-refractory submicron organic mass and black carbon (a tracer of combustion emissions) in the southeastern Pacific that suggest that most of the measured NR-Org was associated with combustion sources.

Several coastal studies reported strong correlations between chlorophyll and the organic fraction of the sea-spray particles for marine periods (Cavalli et al., 2004; O'Dowd et al., 2004, 2015; Ovadnevaite et al., 2014). Shipboard measurements in open ocean conditions from multiple oceans do not support a hypothesized link between primary ocean production and organic enrichment of the aerosol (Beaupré et al., 2019; Kasparian et al., 2017; Keene et al., 2017; Kieber et al., 2016; Quinn et al., 2014, 2019). For example, Quinn et al. (2014) and Bates et al. (2020) used sea sweep (a floating bubbler that generates and samples sea-spray particles) and reported no statistically significant differences in the organic-to-sodium content of the generated submicron aerosol particles in oligotrophic and eutrophic waters in the Western Atlantic and Eastern Pacific oceans. Russell et al. (2010) found that sea-spray organic mass (OM) correlated with local wind speed but not with chlorophyll concentrations for marine periods in the North Atlantic.

There is also a wide range of concentrations reported for the amount of sulfate that can be attributed to marine sources. Some studies found strong correlations between primary productivity and marine sulfate and methane sulfonic acid (MSA) (Mukai et al., 1995; Sciare et al., 2009; Spracklen et al., 2008). Others have reported substantial contributions from sulfate particles transported from the continents to the North Atlantic MBL (Van Dingenen et al., 1995), the Arctic (Frossard et al., 2011), and the northwestern Pacific (Bates et al., 2004; Matsumoto et al., 2004). Zorn et al. (2008) reported a sevenfold increase in sulfate concentrations during continental outflow periods compared to clean Atlantic conditions. Savoie et al. (2002) estimated that 50% to 90% of non-sea-salt sulfate was anthropogenic in origin from several locations in the North Atlantic, with similar conclusions from Van Dingenen et al. (1995). Seguin et al. (2010) and Lin et al. (2012) found that more than 50% of measured sulfur dioxide (SO_2) was biogenic in origin (from DMS oxidation) in the North Atlantic using sulfur isotopic analysis.

Given this variability and uncertainty in attributing submicron particles to specific sources of organic components and sulfate, it is not surprising that there is also a wide range of estimates for how much those specific sources contribute to cloud and climate effects. These effects are controlled by the subset of the submicron aerosol population that serve as nuclei for cloud droplets. Some observations of this subset have shown positive correlations between cloud relevant properties (CCN and cloud droplet concentrations) and primary ocean productivity (Meskhidze & Nenes, 2006; Ovadnevaite, Ceburnis, et al., 2011; Sorooshian et al., 2009). For example, Ovadnevaite, Ceburnis, et al. (2011) found that sea-spray emissions explained 58% of the variability in cloud droplet number concentrations estimated using ground-based remote sensing retrievals at the coastal Mace Head site. Sorooshian et al. (2009) found a positive correlation between CCN and chlorophyll concentrations but not between cloud droplet number and chlorophyll concentrations off the California coast. Sanchez et al. (2018) provided evidence that biogenic sulfate contributions to CCN were much lower in winter (~30%) than in late spring (~60%). Other open ocean measurements of ambient (Quinn et al., 2019) and in situ generated (Bates et al., 2020) aerosol found no direct correlations between CCN concentrations and chlorophyll nor seasonal differences in CCN spectra. At Graciosa Island, Zheng et al. (2018) reported that anthropogenic emissions entrained from the free troposphere were the main source of CCN in the Atlantic MBL, with the highest contribution (~60%) during summer.

This study combines results from complementary chemical measurements from four open-ocean research cruises to characterize the concentrations and sources of submicron particle mass and CCN concentrations in the MBL as part of the North Atlantic Aerosol and Marine Ecosystems Study (NAAMES). NAAMES targeted key events in the annual cycle of phytoplankton biomass in the subarctic Atlantic (Behrenfeld et al., 2019), thus providing a unique dataset to investigate sources of the main particle components in the MBL during and between the winter and late-spring extremes of the annual cycle. Comprehensive atmospheric composition and oceanic measurements between November 2015 and March 2018 provide the ability to attribute sea spray, sulfate, and organic particle mass concentrations and properties to sources, resulting in the first open ocean seasonal budget of submicron particle mass. This budget can then be used to compare the CCN concentrations calculated from chemical components to the observed CCN to assess the role of different components.

2. Methods

2.1. The NAAMES Mission

The NAAMES campaigns targeted key periods of the North Atlantic phytoplankton bloom. The winter campaign (November 2015) occurred during the plankton biomass minimum phase. The late spring campaign (May–June 2016) sampled aerosol during the plankton biomass climax. The autumn campaign (September 2017) targeted the plankton biomass declining phase. Finally, the early spring campaign (March 2018) targeted the plankton biomass accumulation phase. The four NAAMES campaigns were conducted onboard the research vessel *Atlantis*. The latitudinal coverage of the cruises extended between 40°N and 60°N latitudes except for the early spring campaign, which started in San Juan, Puerto Rico (~22°N) and proceeded northward to ~43°N. A detailed description of the NAAMES project, objectives, and atmospheric and oceanic conditions can be found in Behrenfeld et al. (2019).

2.2. Ambient Marine and Continental Periods

Air mass categories were separated into periods of time that were largely marine aerosol sources and periods of time that had substantial continental sources. Ambient marine conditions were defined as periods when (1) particle number concentrations <1,500 cm^{-3}, (2) HYSPLIT 48 hr back trajectories originated from the North or tropical Atlantic and did not pass over land during that time (Figures S1 and S2 in the supporting information), (3) black carbon concentrations (BC, a tracer for combustion) were <50 ng/m^3 (threshold value used by Facchini et al., 2008, and O'Dowd et al., 2014, to remove combustion influences at Mace Head), and (4) radon concentrations typically <500 mBq/m^3. Less than 5% of marine periods during winter and late spring, 10% during early spring, and 20% during autumn had radon concentrations >500 mBq/m^3 but were classified as marine periods because average concentrations for NR-Org, NR-NO_3^-, and BC during these periods were lower than median concentrations for marine periods. Contamination from ship stack emissions was removed by excluding periods of time when the relative wind direction was ±90° from the aft of the ship. This definition of marine periods is similar to that of Saliba et al. (2019) but with the

Table 1
Comparison of Aerosol Properties for the Various NAAMES Campaigns With or Without Additional BC Thresholds to Define Marine Periods

	Winter			Late spring			Autumn			Early spring		
	No threshold	50 ng/m^3	25 ng/m^3	No threshold	50 ng/m^3	25 ng/m^3	No threshold	50 ng/m^3	25 ng/m^3	No threshold	50 ng/m^3	25 ng/m^3
Sampling hours	250	230	200	160	116	80	117	105	83	155	149	106
Number of marine filters for hydroxyl group OM	9	8	6	4	2	2	3	3	2	0	0	0
N_{tot} (cm^{-3}); μ (range)	82 (5–675)	82 (5–675)	77 (5–675)	457 (17–1,500)	383 (17–1,500)	334 (17–1,500)	345 (91–953)	339 (91–953)	324 (91–953)	368 (1–1,240)	368 (1–1,240)	106 (1–1,240)
BC (ng/m^3); μ ± std	17 ± 15	10 ± 11	6 ± 7	35 ± 27	20 ± 16	10 ± 6	25 ± 27	17 ± 13	11 ± 7	22 ± 16	20 ± 12	13 ± 8
NR-org/BC	8.4	15.8	22.6	22	30	57	20	27	42	9.1	9.3	12.8
Hydroxyl group OM/sea salt[a]	0.17	0.17	0.12	0.45	0.49	0.49	0.12	0.12	0.11	N/A	N/A	N/A
NR-Org vs. BC (R value)	0.70	0.70	0.77	0.57	0.40	<0.25	0.36	0.39	0.57	0.68	0.55	0.50
NR-$SO_4^{=}$ vs. BC (R value)	0.59	0.58	0.66	0.58	0.41	<0.25	0.70	0.67	0.71	<0.25	<0.25	<0.25
Non-combustion NR-Org contribution to NR-Org	63%	68%	63%	51%	65%	85%	50%	51%	42%	47%	47%	41%
Non-combustion NR-$SO_4^{=}$ contribution to NR-$SO_4^{=}$	50%	53%	43%	73%	72%	83%	19%	21%	22%	85%	86%	93%

Note. R values rows are shaded by the strength of correlation (not correlated in gray $|R| < 0.25$, light brown for weak $0.25 \leq |R| < 0.5$, and medium brown for moderate $0.5 \leq |R| < 0.8$ (Devore & Berk, 2012).
[a]Sea-salt concentrations are calculated using <1.1 μm size cut filters.

additional BC criterion, which removed ~25% of marine periods for late spring and <10% for the other campaigns (Table 1). Five-day FLEXPART back trajectories for marine periods spent between 81% and 97% of the time over the ocean (Figure S1 in the supporting information).

Continental periods were defined as times when 48-hr back trajectories originated from North America excluding periods of time potentially contaminated by the ship stack emissions. The cumulative distributions of BC, non-refractory organics (NR-Org), and non-refractory sulfate (NR-$SO_4^{=}$) concentrations measured during marine and continental periods (Figure 1) show that the range of concentrations for marine and continental periods sometimes overlaps, such that continental periods include times with concentrations below the median marine concentrations. For instance, between 8% and 13% of the time, BC concentrations during continental periods were as high as median BC concentrations during marine periods, highlighting the contributions of continental or ship sources even during cleaner marine periods. The air mass categories defined here provide a way to separate marine and continental periods, similar to what has been done by O'Dowd et al. (2014), even though marine periods might have some combustion influence. The result is that each campaign includes a different mix of continental and marine sources, which means that the marine periods include some combustion sources that may be either from ships or from the continents.

While the 2-day HYSPLIT and 5-day FLEXPART back trajectories were largely consistent showing little continental influence for marine periods, some influence of transported continental pollution is illustrated by the mean percent time spent over land, which increased from 6.3% (range: 0–9%) for 3-day back trajectories to 13.3% (range: 3–19%) for 5-day back trajectories (see supporting information Text S2 and Table S2). This is consistent with Figure S1, showing that further back in the trajectories there were likely contributions from continental sources, which indicates that the marine periods also had continental contributions. This contribution is probable for particles below 0.5 μm diameter as they can have lifetimes longer than 3 days (Feichter & Leisner, 2009).

2.3. Ambient and Seawater Measurements

Ambient aerosol particles were sampled through a mast inlet positioned about 18 m above sea level, then dried with silica gel driers that were changed approximately every 2–3 days, and then passed to several instruments. The inlet has a transmission efficiency of 95% for particles smaller than 6.5 μm in diameter (Bates et al., 2002) and is equipped with a motor to rotate the nozzle into the wind to ensure isokinetic flow.

High-resolution non-refractory organic mass (NR-Org), sulfate (NR-$SO_4^{=}$), nitrates (NR-NO_3^{-}), ammonium (NR-NH_4^{+}), and chloride concentrations were measured every 5 min using an Aerosol Mass Spectrometer (AMS, Aerodyne Research, Inc., Billerica, MA). NR-$SO_4^{=}$ excludes refractory particles that likely contain the majority of sea-salt sulfate. NR-$SO_4^{=}$ is therefore approximately equivalent to non-sea-salt (nss) sulfate (Frossard, Russell, Massoli, et al., 2014). A 1.0 μm cyclone upstream of the AMS removed supermicron particles. Flow rate, particle size, and ionization efficiency (IE) calibrations

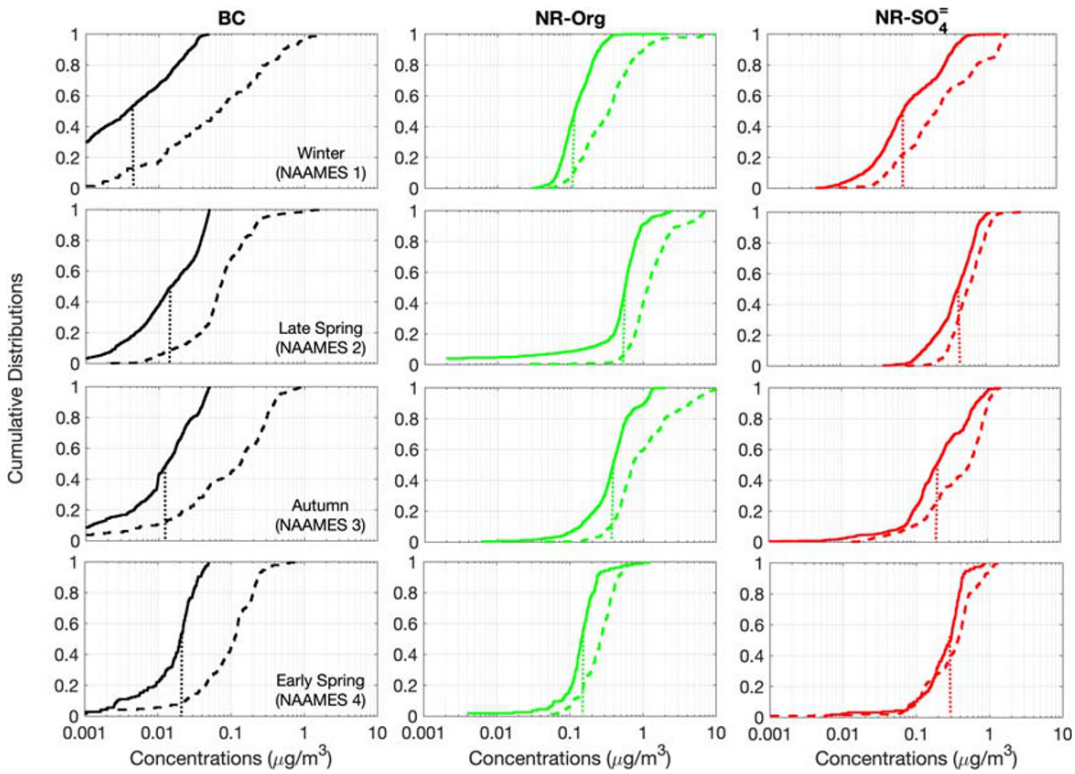

Figure 1. Cumulative distributions for black carbon (BC, left column), non-refractory organic mass (NR-Org, middle column), and non-refractory sulfate (NR-$SO_4^=$, right column). The data are shown for ambient marine periods (solid lines) and continental periods (dashed lines). Vertical dotted lines indicate the median concentrations for ambient marine periods.

were performed prior to and after each campaign. IE calibrations were also completed weekly during the campaigns. The average AMS collection efficiency was calculated for each campaign by constraining to particle size distributions after removing refractory components (see supporting information Texts S3–S6, Figures S3–S10, and Table S3). AMS NR-$SO_4^=$ concentrations were within 10% ($R = 0.84$) of IC nss-$SO_4^=$ after correcting for the AMS collection efficiency (Figure S9 in the supporting information).

Aerosol mobility number size distributions between 0.01 and 1.0 μm were measured using a Scanning Electrical Mobility Spectrometer (SEMS, Model 138, 2002, BMI, Hayward, CA) and a Differential Mobility Particle Sizer (DMPS, TSI) connected to a Condensation Particle Counter (CPC, TSI Inc., St. Paul, MN, model 3781). The accuracy of the size distributions measured by the SEMS was verified using generated polystyrene latex (PSL) particles at diameters 0.1 μm and 0.3 μm prior to each campaign. The peak diameters of the mobility size distributions were within the manufacturer's uncertainty.

Refractory black carbon (BC) number and mass concentrations were measured using a Single Particle Soot Photometer (SP2, DMT, Boulder, CO) for particles between 60 and 700 nm in diameter. The SP2 incandesces individual BC particles using a 1,064 nm laser, and the light emitted is captured by detectors that are calibrated to particle mass (Moteki & Kondo, 2010). The SP2 was calibrated using generated fullerene soot particles prior to and after each campaign, following (Gysel et al., 2011).

Radon (half-life = 3.8 days) was measured by counting radon daughters produced in a 750 L decay tank for a 30-min period (Whittlestone & Zahorowski, 1998).

Submicron inorganic ions including sodium, chloride, sulfate, potassium, and methanesulfonic acid (MSA) concentrations were measured by ion chromatography (IC) (Quinn et al., 1998) from filters that collected ambient air for 12 or more hours, using a two stage multi-jet impactor (Berner et al., 1979). Sea-salt concentrations were estimated as $1.47 \times Na^+ + Cl^-$ (Bates et al., 2012; Frossard, Russell, Burrows, et al., 2014) for the 1.1 μm size cut.

Table 2
Summary of Submicron Speciated Aerosol Measurements for Marine and Continental Periods

Chemical compounds	Measuring instrument	Signature[a]	Origin	Winter μ ± SD (μg/m^3)	Late spring μ ± SD (μg/m^3)	Autumn μ ± SD (μg/m^3)	Early spring μ ± SD (μg/m^3)
NR-Org	AMS[b]	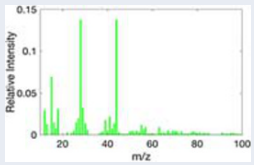	Marine/non-marine	0.14 ± 0.09	0.61 ± 0.39	0.47 ± 0.30	0.15 ± 0.07
		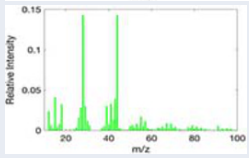	Transported continental	0.56 ± 1.01	1.62 ± 1.43	1.75 ± 2.13	0.27 ± 0.17
		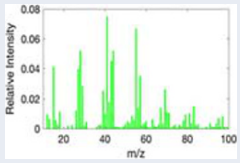	Fresh Combustion	N/A	N/A	N/A	N/A
Hydroxyl	FTIR	-	Sea-spray	0.27 ± 0.18	0.34 ± 0.02	0.08 ± 0.04	N/A[c]
NR-$SO_4^=$	AMS[b]	-	Marine/non-marine	0.15 ± 0.14 (0.48 ± 0.56)	0.44 ± 0.24 (0.64 ± 0.34)	0.36 ± 0.30 (0.52 ± 0.37)	0.27 ± 0.16 (0.39 ± 0.28)
NR-NO_3^-	AMS[b]	-	Mostly non-marine	0.01 ± 0.01 (0.03 ± 0.04)	0.02 ± 0.02 (0.14 ± 0.26)	0.02 ± 0.01 (0.06 ± 0.06)	<0.01 (0.02 ± 0.01)
NR-NH_4^+	AMS[b]	-	Mostly non-marine	<0.01 (0.01 ± 0.15)	<0.01 (0.13 ± 0.15)	<0.01 (0.09 ± 0.10)	<0.01 (0.09 ± 0.11)
BC	SP2	-	Fresh Combustion	0.01 ± 0.01 (0.15 ± 0.25)	0.02 ± 0.02 (0.12 ± 0.21)	0.02 ± 0.01 (0.15 ± 0.15)	0.02 ± 0.01 (0.12 ± 0.11)
MSA	IC	-	Secondary marine	BDL	0.07 ± 0.07 (0.06 ± 0.03)	0.01 ± 0.01 (0.01 ± 0.00)	0.01 ± 0.01 (N/A)
[d]Sea-salt	IC	-	Sea-spray	1.06 ± 0.68	0.41 ± 0.34	0.71 ± 0.52	0.57 ± 0.61
Hydroxyl/[d]sea salt	-	-	-	0.17 ± 0.16	0.49 ± 0.30	0.12 ± 0.01	N/A
CN (cm^{-3})	DMA + CPC	-	-	82 ± 79 (434 ± 483)	383 ± 380 (1,517 ± 1914)	339 ± 202 (673 ± 434)	367 ± 189 (635 ± 477)
$CCN0.1\%_{calc}$ (cm^{-3})	-	-	-	17 ± 13 (53 ± 55)	72 ± 32 (141 ± 76)	60 ± 42 (82 ± 45)	88 ± 57 (124 ± 76)
$CCN0.1\%_{meas}$ (cm^{-3})	CCNC	-	-	18 ± 11 (55 ± 62)	70 ± 37 (100 ± 45)	75 ± 45 (N/A)	82 ± 24 (107 ± 79)
hygroscopicity	-	-	-	0.4 ± 0.0 (0.3 ± 0.0)	0.5 ± 0.1 (0.4 ± 0.1)	0.4 ± 0.1 (0.3 ± 0.1)	0.5 ± 0.1 (0.5 ± 0.1)
$CN_{0.1-0.2}$ $(CCN_{0.1-0.2})_{calc}$	-	-	-	17 ± 4 (4 ± 6)	74 ± 95 (24 ± 13)	71 ± 47 (17 ± 17)	113 ± 63 (52 ± 37)
Wind Speed (m/s)	-	-	-	9.8 ± 3.9 (10.4 ± 4.1)	7.0 ± 4.0 (6.1 ± 2.6)	8.4 ± 3.0 (6.2 ± 2.5)	9.2 ± 3.2 (11.8 ± 4.8)
Chlorophyll (mg/m^3)	-	-	-	0.3 ± 0.2 (0.3 ± 0.4)	1.6 ± 1.2 (1.5 ± 1.3)	0.4 ± 0.2 (0.2 ± 0.2)	0.6 ± 0.3 (0.6 ± 0.4)

Note. Concentrations during continental periods are shown in parentheses except for NR-Org for which marine (first row) and continental (second row) periods are separated. N/A is not available. BDL is below detection limit.
[a]Reference spectra for ambient marine, continental, and ship contamination periods were obtained by averaging AMS unit mass resolution spectra. [b]ACE correction was applied to all AMS concentrations. [c]FTIR filters showed that alkane contribution to FTIR OM greater than 30% suggesting polluted marine conditions. Therefore, hydroxyl group OM concentrations for early spring are not reported. [d]Sea-salt concentrations are calculated using <1.1 μm size cut filters.

Ambient particles were also collected on pre-scanned 37 mm Teflon filters (Pall, Inc., 1 μm pore) for 4 to 24 hr. The collected filters were analyzed offline with Fourier Transform Infrared (FTIR) spectroscopy (Tensor 27 spectrometer, Bruker, Billerica, MA) to determine the submicron organic functional group concentrations (including hydroxyl, alkane, amine, carboxylic acid, and non-acid carbonyl groups). Reported concentrations were background and blank corrected following an automated procedure using prior calibrations (Gilardoni et al., 2007; Maria et al., 2003; Takahama et al., 2013). Sodium concentrations were also measured by IC for a subset of FTIR submicron filters ($N = 12$).

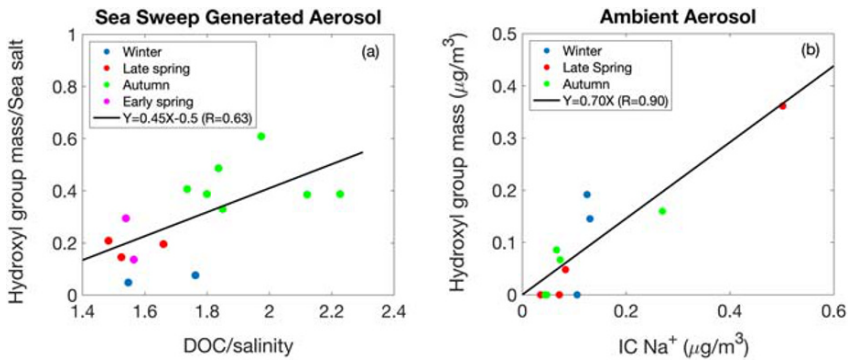

Figure 2. (a) Scatter plot of hydroxyl group OM normalized by sea salt (for <1.1 μm size cut filters) versus seawater DOC concentrations (measured in the first 10 m) normalized to salinity for in-situ generated (sea sweep) aerosol. (b) Scatter plot of hydroxyl group OM versus sodium concentrations for <1.0 μm size cut filters during ambient marine periods. The solid black lines are the lines of best fit obtained using an ordinary least squares regression, and the *p* values are estimated using a two-tailed *T* test.

Shipborne measurements included local true wind speed and chlorophyll concentration (from a pumped seawater supply) along the entire ship track (Table 2). Dissolved organic carbon (DOC) concentrations of the surface seawater (<10 m) were collected by Niskin bottle, filtered in line through a combusted glass fiber filter and measured via the high temperature combustion method using a Shimadzu TOC analyzer (Carlson et al., 2010).

2.4. Organic Mass Concentrations

Sea-spray OM has been shown to be associated with sea-salt particles, given their common origin (Frossard, Russell, Massoli, et al., 2014; Russell et al., 2010). However, sea-spray organic components are mostly missed by the AMS because they are typically on refractory sea-salt particles (Frossard, Russell, Massoli, et al., 2014) which are not efficiently vaporized in the AMS. Sea-spray OM concentrations were estimated as the hydroxyl group OM concentration (C–OH bond) measured by FTIR. The hydroxyl group OM is typical of saccharides and is similar to carbohydrates found in seawater (Russell et al., 2010). We only included samples for which the FTIR spectra and the fractional composition of the sampled marine aerosol were similar to the marine factor identified by Russell et al. (2010) and Frossard, Russell, Burrows, et al. (2014) (Text S4 in the supporting information). For these samples, the hydroxyl group OM accounted for between 75% and 85% of FTIR OM, implying that the hydroxyl group OM could underestimate sea-spray OM by 25% at most. The hydroxyl group OM normalized by sea salt correlated moderately with DOC normalized by salinity (a proxy for DOC normalized by seawater sodium concentrations, $R = 0.63$, $p < 0.05$) for sea sweep aerosol (Figure 2a), consistent with hydroxyl group OM being associated with sea-spray emissions. Here we used the ratio of DOC to salinity instead of just DOC because it was the most analogous metric available to that used for sea spray (from ambient and sea sweep), which was the ratio of hydroxyl group OM to sea-salt mass. Note that the correlation between DOC and hydroxyl group OM normalized by sea-salt mass was similar, with $R = 0.66$ and $p < 0.05$. Ambient hydroxyl group OM correlated strongly with sodium concentrations extracted from the <1.0 μm filters ($R = 0.9$, $p < 0.05$, $N = 12$) during marine periods, suggesting a sea-spray origin for the hydroxyl group OM. Using sodium concentrations collected on <1.1 μm size cut filters, the correlation between hydroxyl group OM and sodium decreased to moderate ($R = 0.55$, $p < 0.05$, $N = 17$, Figure S11). The lower correlation could be due to different size cuts for IC filters (1.1 μm compared to 1.0 μm) and some differences in collection times. Further evidence for the sea-spray origin of the hydroxyl group OM is provided by the lack of correlation between hydroxyl group OM and AMS NR-Org (which is expected if hydroxyl group OM is associated with sea spray and therefore refractory, see supporting information Text S4). For these reasons, the hydroxyl group OM provides a reasonable proxy for sea-spray OM during marine periods. The hydroxyl group OM could not be used as a proxy for sea-spray OM during continental periods because of a contamination of the marine signal with transported non-marine organic sources (which included hydroxyl group OM) that increased the absolute and relative contributions of the alkane group. Therefore, sea-spray OM concentrations for continental periods were assumed to be the

same as those estimated for ambient marine periods for each campaign. This is a reasonable assumption given a similar range of local wind speeds and chlorophyll content for ambient marine and continental periods during each campaign (Table 2).

Using submicron hydroxyl group OM to quantify sea-spray OM means that submicron OM (sea-spray OM and non-refractory OM) would then be the combined organic components from both NR components from the AMS and the FTIR-measured hydroxyl group OM. To avoid double counting the FTIR components that are not associated with sea-spray particles (alkane and carboxylic acid) are excluded. We did not include the alkane group as part of sea-spray OM because the alkane group correlated with BC concentrations (Figure S12 in the supporting information) during marine periods. While some alkane group components are also associated with generated sea-spray aerosol (Frossard, Russell, Burrows, et al., 2014), the contribution of other sources was too large to determine the fraction that should be apportioned to sea spray. The amine group OM correlated strongly with <1.0 μm sodium concentrations ($R = 0.95$, $N = 12$, Figure S13) indicating amine group OM was likely associated with sea spray. However, the statistics are poor because there is only one point each for the winter and autumn for which amine group OM concentrations exceeded the detection limit (Figure S13). Amine group OM was not included as part of the primary sea-spray OM estimate because amine group OM correlated moderately with AMS NR-Org concentrations during winter ($R = 0.6$) and strongly during autumn ($R = 0.85$). The moderate to strong correlation between FTIR amine and AMS NR-Org could also suggest that some of the amine group OM are secondary in origin consistent with recent measurements in the Artic (Köllner et al., 2017) and Antarctic (Liu et al., 2018). Excluding the amine group OM from sea-spray OM does not affect the results reported in this study because amine group OM concentrations were an order of magnitude lower than hydroxyl group OM concentrations. Since AMS misses most refractory OM (which would be on sea-spray particles) and FTIR misses some semi-volatile and Teflon region compounds (which would be included in NR-Org), this combined OM (hereafter "OM") provides a best estimate of all organic components present from marine and continental sources and minimizes double-counting (Text S4 and Figures S4–S6). Since organic carbon (OC) measurements do not account for differences in OM/OC, they are consistent with this approach but do not provide an additional constraint.

3. Seasonal Average Submicron Aerosol Composition

Seasonal average wind speeds and chlorophyll concentrations are shown in Figure 3a. As expected, wind speed was higher during winter and early spring compared to autumn and late spring. In contrast, chlorophyll concentrations peaked during summer and were lower for other seasons.

3.1. Marine Periods

Marine periods contributed between 30% (late spring) and 51% (winter) of the time of each campaign (pie charts, Figure 3). Average submicron aerosol mass concentrations (calculated as the sum of components shown in Figure 3b) varied between 1.0 μg/m^3 (winter, plankton biomass minimum phase) and 1.8 μg/m^3 (late spring, biomass climax phase) for ambient marine periods. The measured range of concentrations is in good agreement with previous measurements in the North Atlantic (Ovadnevaite et al., 2014; Sanchez et al., 2018). The composite annual cycle of the four different seasonal measurement campaigns shows significant seasonal changes in the chemical composition of the submicron aerosol. For example, sea salt accounted for 66% of the submicron mass concentrations during winter but only 22% during late spring, owing to the higher average wind speeds and the lower contributions from other particle sources during winter (Figure 3b). Similarly, organic mass (OM) accounted for 25% of the submicron mass concentrations for winter compared to 52% for late spring.

MSA is the most commonly measured organic compound that serves as a unique tracer for secondary biogenic sulfur in the atmosphere, since its only known marine source to the atmosphere is DMS oxidation. Campaign-averaged MSA concentrations ranged from <0.01 μg/m^3 to 0.07 ± 0.07 μg/m^3 (Quinn et al., 2019) and accounted for between <1% (winter, plankton biomass minimum phase) and 7% (late spring, biomass climax phase) of the submicron OM during ambient marine periods (Table 1). These maximum MSA contributions measured during the plankton biomass climax phase provide an indicator of the magnitude of the DMS contribution to secondary marine organic aerosol formation. The range of <1.1 μm MSA concentrations reported in this study is consistent with the range of submicron MSA concentrations measured at Mace Head (Ovadnevaite et al., 2014) and in the Southern Atlantic Ocean (Zorn et al., 2008), as well as

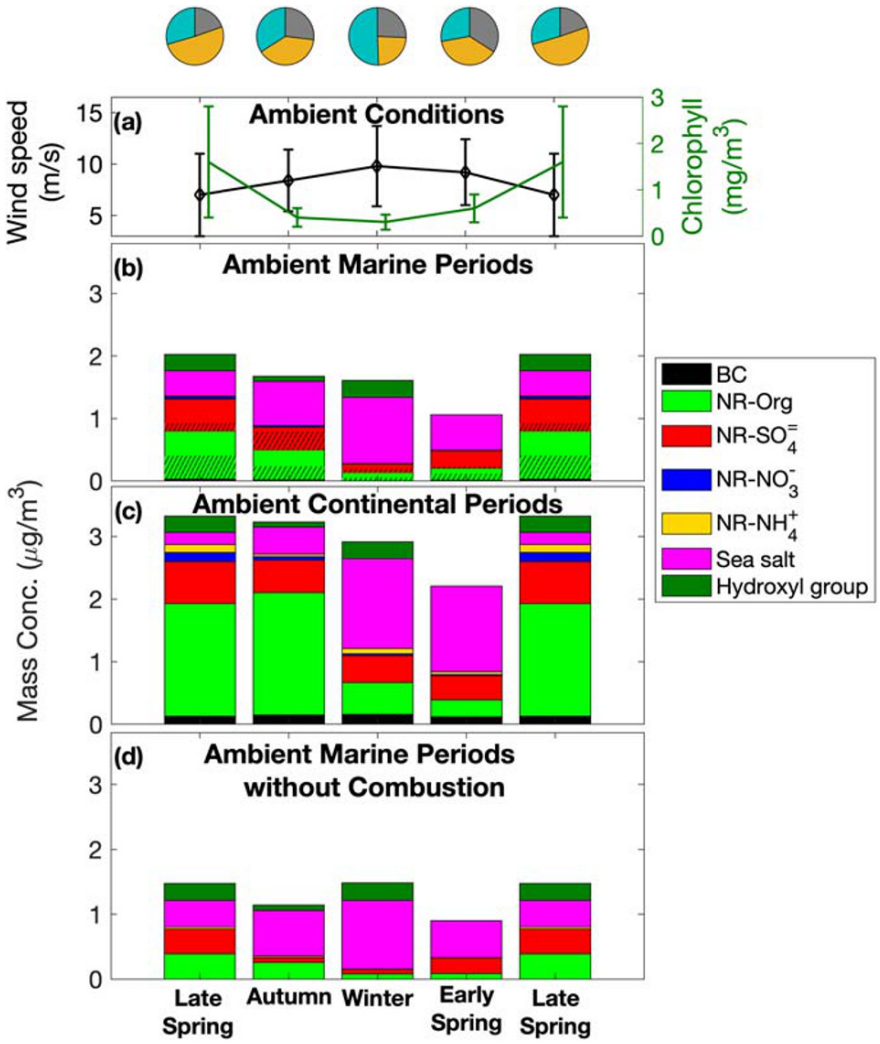

Figure 3. (a) Seasonal average local wind speed (black line, left *y*-axis) and chlorophyll concentrations (green line, right *y*-axis). (b) Seasonal averaged <1.0 μm AMS non-refractory components and FTIR hydroxyl group OM and <1.1 μm sea salt concentrations during ambient marine periods. Hatching indicates an estimate of the anthropogenic contribution to NR-Org and NR-$SO_4^{=}$ (section 4). (c) Continental periods, and (d) ambient marine periods without combustion. Reported concentrations for ambient marine periods without combustion (panel d) were calculated by excluding black carbon (BC), nitrate (NR-NO_3^{-}) and the combustion-related NR-Org and NR-$SO_4^{=}$ from ambient marine periods (hatched areas in panel b). Late spring column is duplicated to better reflect the seasonal cycle. Pie charts at the top indicate the percentage of marine (teal), continental (orange), and potentially contaminated by ship exhaust (grey) periods for each campaign.

with the range of <10 μm MSA concentrations at Cape Grim (Cui et al., 2019), and in the Pacific and Indian Oceans (Saltzman et al., 1983).

NR-$SO_4^{=}$ accounted for between 22% and 27% of submicron mass during ambient marine periods (except for winter which had only 9%). Absolute and relative NR-$SO_4^{=}$ concentrations during ambient marine periods varied significantly by season and were highest during late spring (0.44 ± 0.24 μg/m^3) and lowest during winter (0.15 ± 0.14 μg/m^3), consistent with higher atmospheric DMS concentrations measured during late spring (311 ± 300 pptv) compared to the other campaigns (67 ± 7 pptv in winter, 100 ± 66 pptv in autumn, and 140 ± 36 pptv in early spring), as found previously (Quinn et al., 2019). The seasonal range of NR-$SO_4^{=}$ concentrations reported in this study is comparable to previous measurements in the North Atlantic (Huebert, Zhuang, et al., 1996; Seguin et al., 2011) and the South Pacific (Bates et al., 1992; Jung et al., 2014).

Table 3
Pearson R Values for the Correlations Between AMS NR-Org and NR-$SO_4^=$ With Various Tracers

	Tracer	NR-org				NR-$SO_4^=$			
		Winter	Late Spring	Autumn	Early Spring	Winter	Late Spring	Autumn	Early Spring
Ambient marine	BC	0.70	0.40	0.39	0.55	0.58	0.41	0.67	<0.25
	NR-NO_3^-	0.75	0.57	0.80	<0.25	0.72	0.50	0.45	<0.25
	Radon	0.41	<0.25	<0.25	0.32	0.33	<0.25	−0.42	−0.28
	$C_2H_4O_2^+ + C_3H_5O_2^+$	<0.25	<0.25	0.65	<0.25	0.33	<0.25	<0.25	<0.25
	NR-$SO_4^=$	0.73	0.43	0.26	0.31	-	-	-	-
	MSA	N/A	0.87	<0.25	0.90[a]	N/A	0.64	0.50	0.80[a]
Continental	BC	0.60	0.58	0.81	0.62	0.87	0.33	0.36	0.39
	NR-NO_3^-	0.89	0.89	0.97	0.42	0.36	<0.25	0.26	0.51
	Radon	0.66	0.75	0.63	<0.25	0.35	<0.25	<0.25	<0.25
	$C_2H_4O_2^+ + C_3H_5O_2^+$	0.53	<0.25	0.93	<0.25	<0.25	0.28	0.26	−0.30
	NR-$SO_4^=$	0.33	<0.25	0.28	0.24	-	-	-	-
	MSA	N/A	<0.25	−0.97[a]	N/A	N/A	<0.25	−0.64	N/A

Note. R values reported as N/A are due to MSA concentrations being below detection limit for the winter campaign and not being available during continental periods for the early spring campaign (see Table 2). R values are shaded by the strength of correlation (not correlated in gray $|R| < 0.25$, light brown for weak $0.25 \leq |R| < 0.5$, medium brown for moderate $0.5 \leq |R| < 0.8$, and dark brown for strong $|R| \geq 0.8$ (Devore & Berk, 2012).
[a]The number of points available for the regression was limited to 3.

The moderate to strong ($0.5 < R < 0.8$) correlations observed between MSA and NR-$SO_4^=$ (Table 3) are expected for marine conditions (Choi et al., 2017; Huebert, Wylie, et al., 1996). The lack of very strong correlations shows that there could be some contribution from non-marine sulfate.

Sea-spray OM (approximated as hydroxyl group OM) accounted for 68% of the submicron OM concentration during winter but only 35% during late spring and 15% during autumn. However, sea-spray OM concentrations were highest during late spring (0.33 ± 0.02 μg/m^3, Table 2). The reported range for the relative contribution of sea-spray OM to the total submicron OM during NAAMES (15–68%) is consistent with the value reported by Fu et al. (2011) in the North Atlantic (30% of total OM). Ceburnis et al. (2011) and Miyazaki et al. (2011) reported ratios of sea-spray organic carbon to total carbon of 79% in the coastal northeastern Atlantic and of 88% in the Western North Pacific, respectively. The sea-spray OM-to-sea salt ratio measured during the late spring (plankton biomass climax phase) was a factor of 2.8 to 3.9 larger than in other seasons (Table 2), similar to previous studies of bloom periods (O'Dowd et al., 2004; Ovadnevaite et al., 2014; Zorn et al., 2008). Sea-spray OM contributed 45% of the sum of sea-spray OM and sea salt during late spring compared to <20% for other seasons. However, the higher fraction of sea-spray OM during late spring compared to other seasons was not statistically significant (using a *T*-test at a 0.05 significance level), likely due to the limited number of filter samples during clean marine periods for each campaign ($2 < N < 8$, Table 1). Bates et al. (2020) found no seasonal trends in the OC-to-sodium ratio for sea sweep generated sea-spray aerosol during NAAMES. This difference can be attributed to the sampling of ambient aerosol as opposed to bubble-generated sea-spray aerosol. Sea sweep generated sea-spray aerosol are directly emitted from the ocean and have not interacted with the ambient gases and aerosols. Sea sweep generated aerosol are not influenced by upwind contribution unlike sampled ambient aerosol. Once in the atmosphere the chemical composition of sea-spray aerosol can evolve rapidly through acidification, halogen activation, and organic photochemistry (Keene et al., 2017).

There are few known natural marine sources of nitrate and ammonium in marine aerosol (Harward et al., 1982; Jickells et al., 2003; Quinn et al., 1987). For all NAAMES campaigns, NR-NO_3^- and NR-NH_4^+ contributed <2% of the submicron aerosol composition, consistent with previous measurements (Frossard et al., 2011; Hawkins et al., 2010; Ovadnevaite et al., 2014).

3.2. Continental Periods

BC, NR-Org, and NR-$SO_4^=$ concentrations were higher during continental periods compared to marine periods, as evident by the clear shift in their cumulative distributions at high concentrations (Figures 1 and 3c).

As discussed in section 2.2, NR-Org and BC concentrations for continental periods were lower than median BC concentrations for ambient marine periods between 6.5 and 18% of the time. However, the majority of continental periods had NR-Org and BC concentrations well above the 80th percentile of the ambient marine periods, making the marine and continental periods clearly distinct.

Submicron aerosol mass concentrations were on average a factor of 2 to 3 higher during continental periods compared to ambient marine periods (Table 2), consistent with the expectation that continental sources along the U.S. East Coast and in Europe would contribute sulfate from coal burning, but there were also important differences in aerosol composition. For instance, campaign-averaged BC concentrations were a factor of 6 to 15 times higher during continental periods compared to marine periods. Campaign-averaged submicron OM concentrations were a factor of 1.4 to 3.3 times higher during continental periods compared to marine periods. Non-refractory nitrate (NR-NO_3^-) concentrations were a factor of three to seven times higher during continental periods compared to marine periods. The higher BC, OM, and NR-NO_3^- concentrations from continental relative to marine sources are expected since there are more and larger emissions in close proximity to the coasts (Decesari et al., 2011; Shang et al., 2017). Furthermore, submicron OM consisted largely of NR-Org during continental periods, accounting for 68% of OM for winter, 83% of OM for late spring, and 96% of OM for autumn. The higher contribution of NR-Org to submicron OM during continental periods is not surprising given the additional (likely secondary) organic mass formed and transported from continental outflow. These source apportionments highlight the extent and frequency that non-marine sources of organic particles influenced the open-ocean sampling.

NR-$SO_4^=$ concentrations were also higher by a factor of 1.4 to 3.2 during continental compared to marine periods (Table 2). Only 22% to 37% of the time during continental periods were NR-$SO_4^=$ concentrations below the median NR-$SO_4^=$ concentrations for ambient marine periods (Figure 1). This indicates clear transport of NR-$SO_4^=$ from the continents, consistent with Zorn et al. (2008) and Simpson et al. (2014), who found higher sulfate concentrations in the North Atlantic during continental outflow periods compared to marine periods. Similar findings were also reported in the subtropical Atlantic (McGovern et al., 1999) and in the southeastern Pacific Ocean (Hawkins et al., 2010).

Interestingly, sea-salt concentrations were higher during continental periods compared to marine periods during winter (35%, Figure 3c) and early spring (140%, Figure 3c). This difference in sea-spray concentrations may be associated with the coincidentally higher local mean wind speeds measured during winter and early spring for continental periods (10.4 and 11.8 m/s) compared to marine periods (9.8 and 9.2 m/s) (Table S1).

4. Sources of Submicron Aerosol Particles

Campaign-averaged submicron non-refractory organic mass spectra for marine and continental periods were too similar to use to distinguish sources. The few AMS fragments that differed (m/z 73, 83, and 98) were not useful tracers for specific sources (e.g., m/z 43, 44, 57, and 60; Aiken et al., 2009; Zhang et al., 2005) (see supporting information Text S7, Table S4, and Figures S14–S16). The mass spectra of NR-Org were generally very similar (Figure S14 in supporting information). For these reasons, relationships to non-AMS tracers are used to distinguish sea spray and secondary organic and sulfate sources.

4.1. Tracers for Sea-Spray Organic Sources

The strong and positive correlation between sea-spray OM concentrations (approximated by the FTIR hydroxyl group OM) and IC sodium concentrations (both from <1.0 μm filters, $R = 0.9$, $p < 0.05$, Figure 2b) provides evidence of a marine source of the hydroxyl group OM. For all NAAMES campaigns, the hydroxyl group OM did not correlate with BC (Figure S5 in the supporting information) or with incident short wave radiation ($R < 0.2$), making it unlikely that hydroxyl group OM was related to combustion or was secondary. A sea-spray source of OM is also indicated for the sea sweep bubble-generated aerosol by the moderate correlation of the ratio of hydroxyl group OM to sea-salt concentrations with the ratio of DOC concentrations to salinity ($R = 0.63$, $p < 0.05$, Figure 2a). This relationship indicates that sea spray is the likely source of much of the hydroxyl group OM.

NR-Org concentrations (which were higher than sea-spray OM concentrations for all seasons except for winter) did not correlate with wind speed or sea salt, which implies that NR-Org was likely not associated with

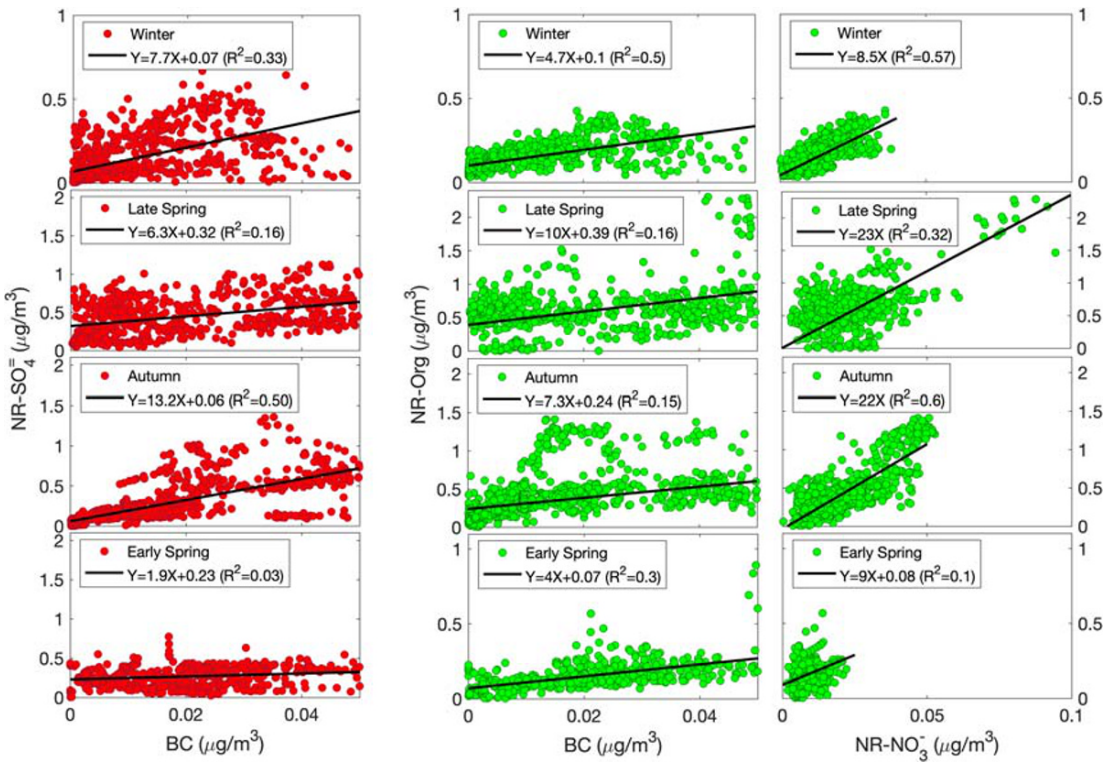

Figure 4. Scatter plot for (left column) NR-$SO_4^{=}$ versus BC, (middle column) NR-Org versus BC, and (right column) NR-Org versus NR-NO_3^{-} in submicron aerosol during ambient marine periods. The panels show the four NAAMES campaigns. Solid black lines are the lines of best fit obtained using an ordinary least squares regression.

sea-spray OM. To identify the source of NR-Org, BC was used as a tracer for primary combustion particles and regressed against NR-Org. BC explains between 15% (autumn) and 50% (winter) of the variability in NR-Org during ambient marine periods (Figure 4). The relative-standard deviation (standard deviation [σ] divided by mean [μ]) varied from 47% to 64% for NR-Org during marine periods. Hence, the weak to moderate BC correlations indicate a contribution of combustion emissions to the NR-Org during the marine periods, even though this is not the case for the hydroxyl group OM. The correlation between NR-Org and BC do not imply that all NR-Org is from primary combustion since NR-Org can also form through secondary oxidation of combustion and non-combustion organic vapor precursors. Some NR-Org may also be associated with sea-spray OM (Frossard, Russell, Massoli, et al., 2014), although for NAAMES that contribution is not large enough to result in significant correlations.

The ratio of NR-Org to BC ranged from 9.3–30 for ambient marine periods and 2.2–13.8 for continental periods. Historically, a version of this ratio has been used to track the relative amounts of combustion and secondary contributions to OM. For comparison, the ratios for ambient marine periods (9.3–30) are generally lower than those reported at Mace Head during clean marine conditions (range: 28–182) (O'Dowd et al., 2014). The lower ratios measured during NAAMES imply a higher contribution from combustion sources during ambient marine periods compared to other campaigns. This range is higher than values of 5–13 reported for ship emissions (Betha et al., 2017; Moldanová et al., 2009), consistent with a higher non-combustion marine source. In addition, the continental periods are also lower than those reported from coastal measurements in the northeastern U.S. coast (ratio = 34) during continentally influenced periods of northwesterly flow (Bates et al., 2005). The lower ratio during continental periods compared to ambient marine periods is consistent with higher marine contributions during marine periods and closer to OC-to-EC values of 2.5–3.6 found for continental outflow in the northwestern Pacific (Lim et al., 2003).

The strength of the correlations between NR-Org and BC was weaker during marine periods ($0.39 < R < 0.70$, Table 3) than during continental periods ($0.58 < R < 0.81$). The correlations reported for marine periods in this study are weaker than the strong correlation ($R = 0.81$, slope = 14) reported in the

southeastern Pacific, even when BC concentrations were below 20 ng/m^3 (Shank et al., 2012). This likely implies smaller contributions from ship traffic emissions during marine periods during NAAMES compared to VOCALS.

4.2. Tracers for Secondary Organic Sources

The weak to moderate correlations between NR-Org and BC imply that some part of the NR-Org was associated with combustion but not all. NR-Org correlated significantly and strongly ($R > 0.89$, Table 3) with NR-NO_3^- (a product of secondary production from NO_x; Seinfeld & Pandis, 2006) during continental periods, except for early spring for which the correlation was weak ($R = 0.42$). The co-variation of NR-Org and NR-NO_3^- could reflect simultaneous emission of precursor NO_x and organic vapor gases and photochemical production of these aerosol components from oxidation. Since the nitrate precursor is likely NO_x transported from continental sources, the correlation of NR-Org with NR-NO_3^- suggests that the NR-Org precursors may well also have a continental origin. This is further supported by the moderate correlations ($0.63 < R < 0.75$, Table 3) between NR-Org and radon for continental periods (but not for marine periods), except during early spring for which the two were not correlated.

Similarly, NR-Org and NR-NO_3^- correlated moderately during late spring ($R = 0.57$, Table 3) and winter ($R = 0.75$) and strongly during autumn ($R = 0.80$) for marine periods but did not correlate during early spring. This suggests that secondary organic mass may also form from continental sources during marine periods. The range of the NR-Org/NR-NO_3^- ratio during marine periods (8.5–24, Figure 4) is consistent with previous measurements from the northeastern United States and Canada (Jimenez et al., 2009) and from the North Atlantic (Ovadnevaite et al., 2014) and is larger than the ratio of ~2 expected in regions with high NO_x emissions (e.g., Southern California, Jimenez et al., 2009). Regressions for NR-Org versus NR-NO_3^- had zero y-intercept values during ambient marine periods (Figure 4, except for early spring), consistent with the majority of NR-Org being secondary. Since MSA is known to be marine and secondary in origin (Jefferson, 1998), the strong correlations between NR-Org and MSA concentrations (Table 3) during ambient marine periods for late spring ($R = 0.87$) and early spring ($R = 0.90$) suggest that the NR-Org also has a marine source and a secondary formation mechanism. This is expected since NR-Org has been shown to include some MSA-related fragments (Hodshire et al., 2019).

During autumn NR-Org correlated strongly ($R = 0.93$, Table 3) with mass fragments that have been used as biomass burning tracers (sum of $C_2H_4O_2^+$ at m/z 60 and $C_3H_5O_2^+$ at m/z 73; Alfarra et al., 2007) for continental periods and moderately ($R = 0.65$) for marine periods. This indicates a contribution from biomass burning emissions from North America (Figures S1 and S17) during autumn. However, the median value for the fractional contribution of fragment $C_2H_4O_2^+$ (m/z 60) was lower than the background level of 0.3% reported during the ARCTAS mission (Cubison et al., 2011) (Figure S18). Moreover, the fit for the NR-Org versus the sum of $C_2H_4O_2^+$ and $C_3H_5O_2^+$ had a zero y-intercept, suggesting a small contribution of regional marine sources to NR-Org for autumn during continental periods. The attribution of NR-Org to biomass burning emissions during autumn is further supported by the moderate correlation between NR-Org and submicron non-sea-salt potassium ion concentrations (K^+, $R = 0.70$, $p < 0.05$). Contributions of biomass burning emissions to particles in marine areas have been previously reported (Choi et al., 2017; Kanitz et al., 2013; Virkkula et al., 2006).

The lines of best fit for NR-Org and BC during ambient marine periods have positive y-intercept values. Cabada et al. (2004) used the intercept of the regression of OC to EC to represent the "noncombustion organic carbon" contribution to the primary OC concentration, consistent with the previous work of Lim and Turpin (2002) who used the y-intercept of OC regressed to CO as an indicator of primary OC. Here we interpret the y-intercept of NR-Org with BC to indicate a non-combustion component of secondary sources of NR-Org that are either marine or continental (vegetation) in origin. With this method, the contribution from non-combustion sources for NR-Org were (average ± 95% confidence bounds) 68 ± 4% for winter (0.10 μg/m^3), 65 ± 7% for late spring (0.39 μg/m^3), 51 ± 7% for autumn (0.24 μg/m^3), and 47 ± 7% for early spring (0.07 μg/m^3) (Figure 4). The remaining 36% of the NR-Org (but only 27% of submicron OM) measured as the NAAMES campaign averages for marine periods is inferred to be associated with combustion.

The low amounts of BC and nitrate during marine periods provide an apparent contradiction to the moderate correlations of these components to NR-Org, as expected since correlation does not imply source

attribution if the NR-Org is not from a single source. For this reason, we also used positive matrix factorization (PMF) to separate NR-Org by sources, but there were not enough source specific fragments or enough dynamic range of different source contributions to provide a robust separation beyond the tracer regression method presented in Table 3 (see supporting information Text S7).

4.3. Tracers for Secondary Sulfate Sources

AMS NR-$SO_4^=$ correlated weakly to strongly with NR-NO_3^- and MSA concentrations during ambient marine periods (Table 3), consistent with a similar precursor of NR-$SO_4^=$ and MSA (DMS) and a similar formation process (photooxidation) with NR-NO_3^-. The weakness of the correlation between NR-$SO_4^=$ and NR-NO_3^- could result from the differences in NO_2 and DMS lifetimes. Similar correlations between MSA and NR-$SO_4^=$ have been observed in the coastal northeastern Atlantic (Ovadnevaite et al., 2014), in the equatorial Pacific (Huebert, Wylie, et al., 1996), in the North Pacific (Choi et al., 2017), and South Pacific (Savoie et al., 1994). The higher NR-$SO_4^=$ concentrations measured during continental periods compared to marine periods (Table 2) indicate that DMS oxidation is not the only source of sulfate particles to the MBL. Long-range transport of NR-$SO_4^=$ may also contribute to the observed concentrations during marine periods, although the correlations between NR-$SO_4^=$ and BC for continental periods were weak during spring and autumn (Table 3 and Figure S19). The weak correlations between NR-$SO_4^=$ and BC are expected since BC is primary whereas sulfate is secondary. A higher biogenic contribution to NR-$SO_4^=$ during continental periods compared to marine periods for late spring and autumn cannot be ruled out (Table S5 in the supporting information). BC explained between 3% and 50% of the variability of NR-$SO_4^=$ for ambient marine periods (Figure 4). If the *y*-intercept value of the NR-$SO_4^=$ for the linear regression to BC is interpreted as the non-combustion contribution to NR-$SO_4^=$ then non-combustion sources contributed (average ± 95% confidence bounds) 53 ± 8% of NR-$SO_4^=$ during winter, 72 ± 7% during late spring, 21 ± 5% during autumn, and 86 ± 7% during early spring for marine periods, consistent with the large range of the biogenic contribution to sulfate concentrations in the MBL (10–80%) reported over the North Atlantic (Lin et al., 2012; Savoie et al., 2002). The ratio of MSA to MSA + non-combustion NR-$SO_4^=$ was 14% in autumn, 22% in late spring, and only 4% in early spring. The autumn and late spring ratios are close to the 15% MSA to MSA + SO_2 expected from DMS oxidation obtained from a global chemical transport model (Chen et al., 2018). The ratios of MSA to MSA + non-combustion NR-$SO_4^=$ measured during the NAAMES campaigns are within the range (<5–25%) reported from several locations (Ayers et al., 1991; Bates et al., 1992; Savoie et al., 2002), providing further support for the fraction of sulfate apportioned as biogenic during ambient marine periods.

NR-$SO_4^=$ correlated moderately with BC only during winter ($R = 0.58$) and autumn ($R = 0.67$) for ambient marine periods (Table 3). These correlations could point to particles from nearby ship emissions. Another explanation could be the coincident transport of BC and NR-$SO_4^=$ from the free troposphere. In contrast, the elevated NR-$SO_4^=$ concentrations measured during early spring (plankton biomass accumulation transition) and late spring (biomass climax) did not correlate with BC concentrations for early spring and correlated weakly for late spring, consistent with a marine source of sulfate particles.

4.4. Seasonal Cycle of Submicron Aerosol Excluding Combustion Influence

To estimate the seasonal concentrations of non-combustion submicron components during ambient marine periods, the positive *y*-intercept values from regressing AMS components versus BC (sections 4.2 and 4.3) during ambient marine periods were subtracted from their seasonal mean concentrations (Figure 3d). BC and NR-NO_3^- were excluded since they have little to no marine non-combustion sources. After removing combustion components, submicron particle mass concentrations were reduced from 1.0–1.8 to 0.9–1.5 $\mu g/m^3$, but the variability remained the same (RSD = 20%, Figure 3). There were seasonal differences for some of the submicron non-refractory components. Seasonal non-combustion (likely biogenic) NR-Org and NR-$SO_4^=$ concentrations were highest during late spring (0.39 $\mu g/m^3$ for NR-Org and 0.32 $\mu g/m^3$ for NR-$SO_4^=$) and lowest during winter (0.1 $\mu g/m^3$ for NR-Org, 0.07 $\mu g/m^3$ for NR-$SO_4^=$). This result agrees with previous studies that indicate enhanced marine biogenic emissions during bloom periods (O'dowd et al., 2015; Ovadnevaite et al., 2014; Sciare et al., 2009).

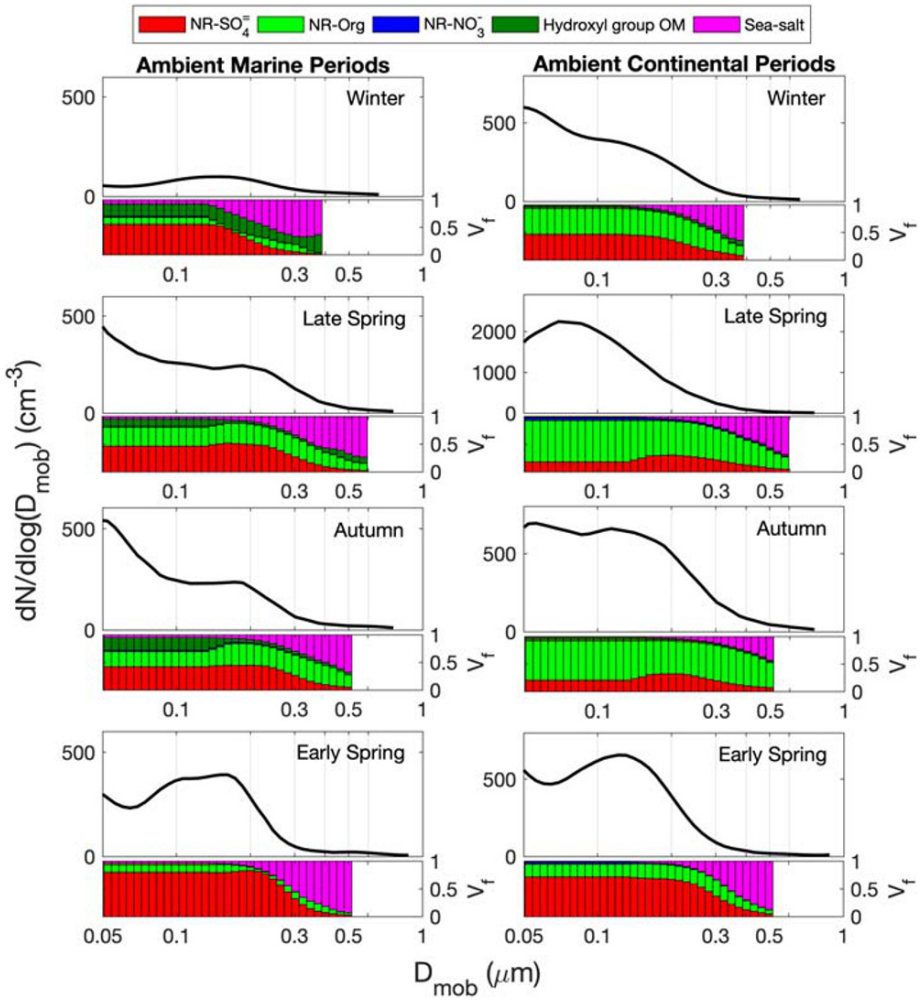

Figure 5. Campaign-averaged electrical mobility number size distributions (solid black lines) for ambient marine periods (left column) and continental periods (right column). Also shown below each size distribution plot are the campaign-average fractional volume contributions (V_f) for non-refractory sulfate (NR-$SO_4^{=}$), non-refractory organic mass (NR-Org), nitrate (NR-NO_3^{-}), sea salt, and the hydroxyl group OM (a proxy for sea-spray OM) when available. Note the differences in the *y*-scale for late spring continental periods. AMS PToF vacuum aerodynamic size distributions and FTIR hydroxyl group OM aerodynamic size distributions were both adjusted to mobility diameters.

4.5. Effects of BC Criteria for Marine Periods

Since the choice of the BC threshold is arbitrary, three different criteria were analyzed: (1) a BC threshold of 50 ng/m^3 as used in this study (base case, BC50), (2) a stricter BC threshold of 25 ng/m^3 (BC25), similar to Quinn et al. (2019), and (3) no BC threshold (no threshold), similar to Saliba et al. (2019) (Table 1). The number of hours of measurements for each campaign that fit the criteria decreased from 117–250 hr for no threshold to 105–230 hr for BC50 and to 80–200 hr for BC25. Campaign-averaged particle number concentrations decreased from 82–457 cm^{-3} for no threshold to 82–383 cm^{-3} for BC50 and 77–334 cm^{-3} for BC25, although the range of particle number concentrations was unchanged for the three cases (Table 1).

The ratio of NR-Org to BC increased for BC50 (range = 9.3–30) and BC25 (range = 12.8–57) compared to no threshold (range = 8.4–22) (Table 1). The higher NR-Org to BC ratio for the stricter BC50 and BC25 thresholds did not result in a consistent decrease in the strength of the correlation between the two, which would be expected if the source for the majority of the NR-Org components were non-combustion. During late spring, the correlation between NR-Org and BC decreased from moderate (no threshold) to weak (BC50) to not correlated for BC25. The correlation between NR-Org and BC was moderate for all three cases

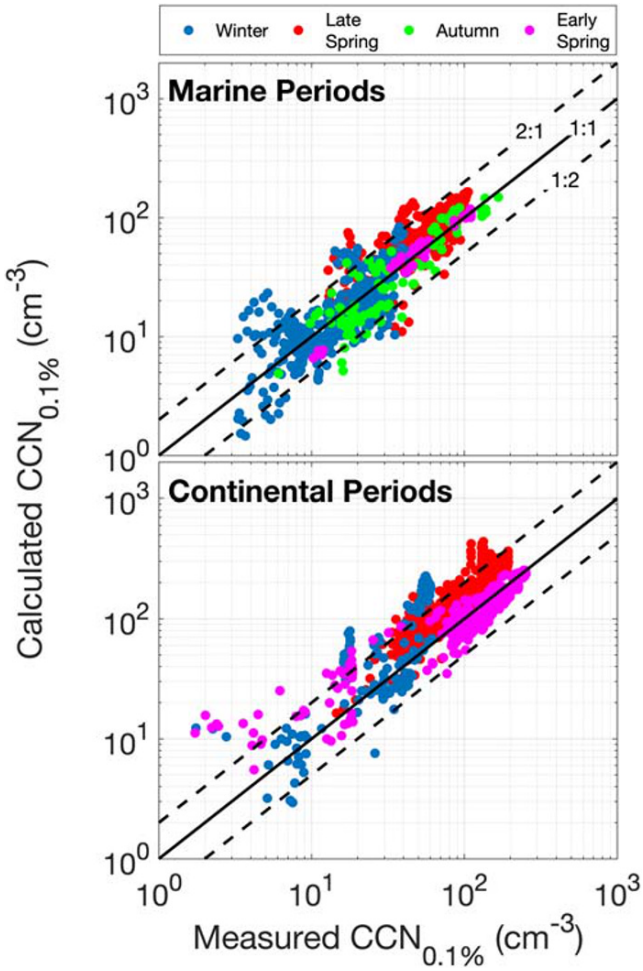

Figure 6. Comparison of measured and calculated CCN concentrations at 0.1% supersaturation during marine periods (top) and continental periods (bottom). The data are colored by campaign. The solid black line is the 1:1 line and the dashed black lines are the 1:2 and 2:1 lines.

during early spring and winter and increased from weak (no threshold and BC50) to moderate (BC25) during autumn (Table 1). A stronger correlation between NR-Org and BC during marine periods defined to be even cleaner (e.g., BC < 20 ng/m^3) was reported by Shank et al. (2012).

Three campaigns (winter, autumn, and early spring) had no change for stricter BC thresholds, indicating that the identified trends in NR-Org and NR-$SO_4^=$ were generally consistent even when times with more combustion were removed (Table 1). One campaign (late spring) shows weaker correlations for stricter BC criteria, indicating that the trend was not consistent when times with more combustion were removed. This could be because late spring had the largest contribution from non-combustion NR-Org and NR-$SO_4^=$, meaning that there was enough non-combustion NR-Org and NR-$SO_4^=$ to overwhelm the combustion-driven correlations.

The percent NR-Org and NR-$SO_4^=$ attributed to non-combustion sources generally varied by <10% for stricter BC thresholds during winter, autumn, and early spring (Table 1). This indicates that the values reported in Table 1 were not very sensitive to the BC threshold chosen. For late spring, the increase in the fraction of NR-Org attributed to non-combustion from 51% for no threshold to 65% for BC50 and 85% for BC25 could indicate that stricter BC thresholds are removing additional combustion-related NR-Org components for that campaign.

There were no notable changes to the ratio of hydroxyl group OM (a proxy for sea-spray OM) to sea-salt concentrations for ambient measurements among all three cases. This lack of sensitivity of the hydroxyl group OM to BC is further evidence that hydroxyl group OM is not related to combustion during marine periods.

In summary, the BC50 threshold for marine periods provided a good balance between removing the majority of combustion sources (including some ships) and retaining sufficient sampling times to represent the variability in each campaign. For these reasons, the BC50 threshold was used as the primary focus of this work.

5. Size Distributions and CCN Implications

Seasonal changes in the chemical composition of the submicron aerosol are important for estimating CCN, especially for the 0.1–0.2 μm size range for which the hygroscopicity of the aerosol is sensitive to its chemical composition (Quinn et al., 2008).

5.1. Particle Number and Chemical Size Distributions

The campaign-averaged particle number size distributions and their fractional chemical composition are shown in Figure 5 for marine and continental periods (see supporting information Figures S20 and S21 and Tables S5 and S6 for mass size distributions). The AMS PToF signal for NR-NH_4^+ and Cl^- was negligible and was not included. Sea salt was estimated from fitting the larger tail (dry mobility diameter >0.6 μm) of hourly averaged particle number size distributions (Saliba et al., 2019). The <0.18, <0.5, and <1.0 μm aerodynamic filter cuts for hydroxyl group OM were used to construct a 3-bin size distribution for sea-spray OM. The relative composition of the <0.18 μm aerodynamic diameter (~0.14 μm mobility diameter) was held constant because FTIR was measured on <0.18 μm aerodynamic diameter size cut filters and because the AMS signal was not strong enough to give reliable NR-Org and NR-$SO_4^=$ mass size distributions for <0.1 μm (Figure 5). For the 0.18–0.5 and 0.5–1.0 μm aerodynamic diameter ranges, the hydroxyl group OM concentration was held constant but AMS mass concentrations and sea-salt concentrations varied with the

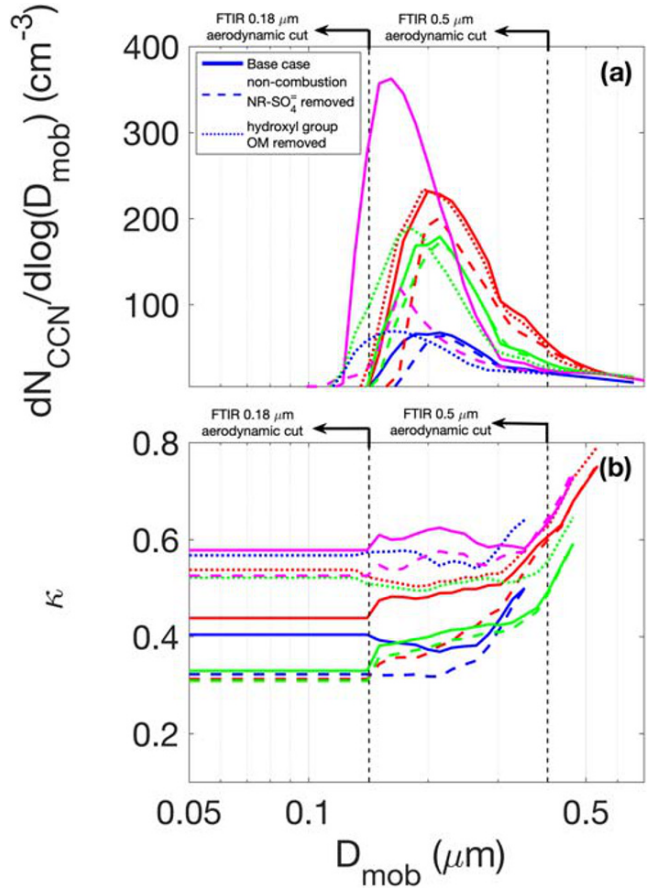

Figure 7. (a) Campaign-averaged CCN number mobility size distribution for all NAAMES campaigns during ambient marine periods (base case, solid lines). (b) Size-dependent hygroscopicity parameter (κ, calculated at 0.1% supersaturation and assuming internal mixture of all compounds) for all NAAMES campaigns (base case). Also shown on (a) and (b) are calculations excluding the FTIR hydroxyl group OM (a proxy for sea-spray OM, dotted lines) when available (Table 1) and excluding the non-combustion NR-$SO_4^{=}$ (dashed lines). Blue colored lines are for winter (NA1), red for late spring (NA2), green for autumn (NA3), and magenta for early spring (NA4). FTIR aerodynamic size cuts for hydroxyl group OM are shown as dashed vertical lines.

measured distributions. This assumption is justified given that the fractional contribution from hydroxyl group OM for 0.18–0.5 and 0.5–1.0 μm aerodynamic diameters was small (<20% during winter and <10% for the other seasons, Figure 5).

Campaign-averaged submicron number size distributions were mostly bimodal with one peak at dry mobility diameter <0.05 μm and the second peak in the 0.1 to 0.2 μm accumulation mode range (Figure S21 in the supporting information). For all campaigns, at sizes >0.3 μm sea salt accounted for between 50 and 90% of the mass and NR-$SO_4^{=}$ accounted for <10% of the mass (Figure 5). During marine periods, NR-$SO_4^{=}$ contributed ~50% of the mass in the 0.1–0.2 μm mobility diameter range during winter and late spring and as high as 80% during early spring. The contribution was lowest (~40%) during autumn. For winter, sea salt contributed between 20% and 30% of the mass in the 0.1–0.2 μm diameter range, consistent with low aerosol concentrations and higher average local wind speeds, while the contribution of sea-salt particles was negligible for the other three NAAMES campaigns.

During continental periods, NR-Org provided between 50% and 75% of the mass in the 0.1 to 0.2 μm mobility diameter range (except during early spring, Figure 5), consistent with more volatile organic carbon emissions from the continents that are oxidized during transit over the ocean. At sizes >0.3 μm mobility diameter, sea salt contributed 50% to 75% of the mass except during autumn for which sea salt contributed <30% of the mass. The large contribution of NR-Org to the mass of particles >0.3 μm during autumn (Figure 5) could be associated with transport of biomass burning emissions to the MBL (Table 3), since particles from biomass combustion are often larger than those from other combustion sources (Betha et al., 2018).

5.2. Potential Implications for CCN Concentrations in the MBL

CCN concentrations (Table 1) were calculated using the measured aerosol chemical composition, assuming a complete internal mixture with size resolved composition, supersaturations of 0.1%, 0.2%, and 0.3%, and a constant surface tension (0.072 J/m^2). Hourly averaged AMS composition measurements, sea-salt measurements estimated from fitting hourly-averaged particle number size distributions (Saliba et al., 2019), and FTIR hydroxyl group OM concentrations were used to calculate size-resolved kappa (κ) values. Assuming that the variability in sea-spray OM over filter sampling periods can be approximated by the variability in sea-salt concentrations over the same periods and that sea-spray OM concentrations are constant for the filter sample durations (but hourly varying AMS composition and sea salt) does not account for an additional 35% variability (see Text S8 in supporting information for more details). For this calculation, κ values of 0.7 for NR-$SO_4^{=}$, 1.1 for sea salt, and 0.1 for NR-Org and hydroxyl group OM were used for hygroscopicity (Mochida et al., 2011; Moore et al., 2011; Sanchez et al., 2018; Schill et al., 2015; Sullivan et al., 2010). The surface tension may also be reduced by organic components, which could offset the reduction in hygroscopicity, but that effect is not reflected in these calculations.

For all NAAMES campaigns, the average calculated CCN concentrations were within one standard deviation (which were 29 to 69%) of the average measured CCN concentrations at 0.1% supersaturation reported by Quinn et al. (2019) for marine periods. The average calculated and measured CCN concentrations at 0.1% supersaturation during marine periods were within 30% for all campaigns (Table 2 and Figure 6), demonstrating that the combined AMS, FTIR, and salt particle estimates provide reasonable CCN concentrations from this "bottom-up" calculation, similar to the degree of agreement found by past closure studies (Moore et al., 2012; Roberts et al., 2006; Wex et al., 2010). Calculated and measured CCN concentrations

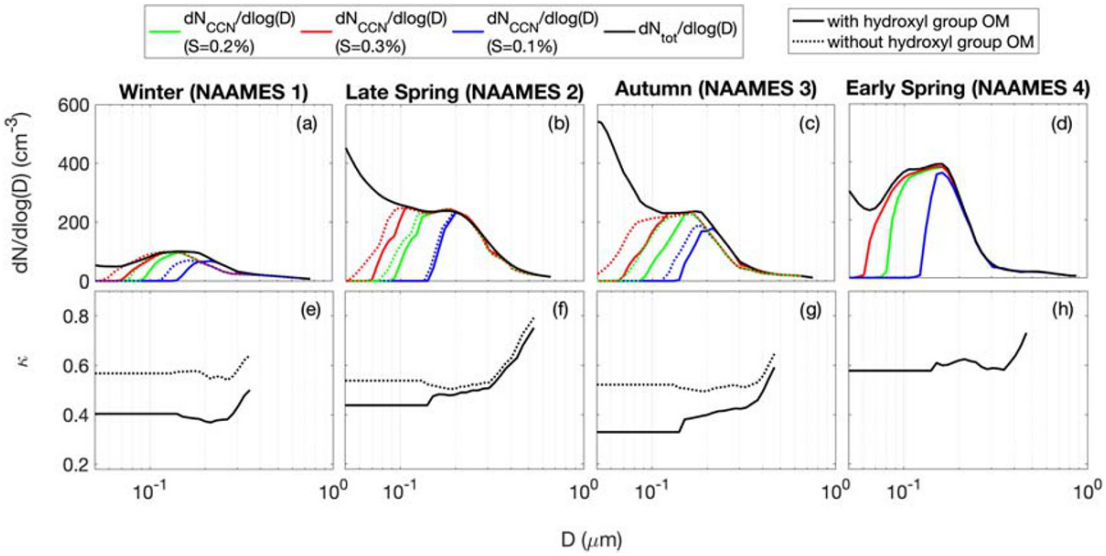

Figure 8. (a–d) Average particle mobility number size distributions for ambient marine periods (solid black lines) and CCN number size distributions (colored lines) calculated at different supersaturations (S). (e–h) Hygroscopicity (κ) as a function of mobility particle size calculated using complete chemical composition (solid lines) and after excluding the hydroxyl group OM when available (dotted lines), assuming complete internal mixture. Solid and dotted lines in panels a–d represent CCN number size distributions calculated with and without hydroxyl group OM respectively.

for continental periods were within one standard deviation of one another (Table 2 and Figure 6), except for late spring for which calculated CCN concentrations overestimated measurements by 52%. CCN concentrations calculated assuming an external mixture have been found to be generally lower than CCN concentrations calculated assuming an internal mixture (Schill et al., 2015). Therefore, the large measurement variability and the lower measured CCN compared to CCN calculated for an internal mixture for late spring could reflect a particle population that is externally mixed during continental periods. For marine periods, campaign-averaged calculated CCN concentrations at 0.1% supersaturation were higher during late spring (72 ± 32 cm^{-3}) and early spring (88 ± 57 cm^{-3}) than during winter (18 ± 13 cm^{-3}) and autumn (60 ± 42 cm^{-3}). Using calculated CCN concentrations, the fraction of CN particles that were CCN at 0.1% was nearly constant at ~0.2 for marine periods during all four seasons (Table 2).

The factor of ~1.5 higher CN concentrations in the 0.1–0.2 μm mobility size range during early spring compared to late spring and autumn did not result in a similar increase in CCN concentrations in that size range (Table 2). CCN concentrations at 0.1% supersaturation in the 0.1–0.2 μm mobility diameter range during early spring were a factor of 2.2 and 3.1 higher than late spring and autumn, respectively. The higher CCN/CN fraction during late spring is due to the higher hygroscopicity during early spring in the 0.1–0.2 μm mobility diameter range (Figure 7).

The effects of non-combustion sulfate and OM components on calculated particle κ and CCN concentrations as functions of particle size are shown in Figure 7 for ambient marine periods (see supporting information Figure S22 for continental periods). Calculated κ generally increased with particle size as expected, consistent with higher contributions from OM at smaller sizes and higher NR-$SO_4^=$ and sea salt at larger sizes (Figure 5). However, κ was larger at smaller sizes for early spring due to a large contribution from NR-$SO_4^=$ at these sizes (Figure 5) and decreased between 0.14 and 0.30 μm due to a larger contribution from OM. The sensitivity of κ and CCN concentrations to sea-spray OM and non-combustion, likely biogenic, NR-$SO_4^=$ was investigated by removing the contribution of each component to κ and CCN. Removing each component resulted in changes to the particle hygroscopicity and a shift of the particle number size distribution to smaller sizes. Removing sea-spray OM consistently increased campaign-average κ by 41% (winter), 10% (late spring), and 35% (autumn) but resulted in <10% increase in CCN concentrations at 0.1% supersaturation (Figure 7). In contrast, removing non-combustion, likely biogenic, NR-$SO_4^=$ decreased κ by 7% (autumn) to 20% (late spring) and resulted in decreased CCN concentration between 7% (autumn) and

66% (early spring) at 0.1% supersaturation (Figure 7). These results show that the main effect of seawater biology on aerosol-cloud interactions at 0.1% is the addition of biogenic (non-combustion) sulfate, which increases hygroscopicity (by more than it is decreased by adding sea-spray OM) and increases the number of particles large enough to serve as CCN (~0.1 μm). At 0.1% supersaturation, calculated CCN number concentrations for particles >0.2 μm were independent of their hygroscopicity because all particles >0.2 μm in diameter activated (Figure 8), assuming the measured chemical composition was internally mixed.

Higher supersaturations (0.2–0.3%) are sometimes more relevant in the MBL (Hoppel et al., 1996; Snider et al., 2003). At a supersaturation of 0.3%, CCN number concentrations were higher than at 0.1% supersaturation by 97% (late spring) and 120% (autumn) (Figure 8). At 0.3% supersaturation, replacing sea-spray OM with hygroscopic sulfate increased CCN number concentration by <5% during winter, late spring, and early spring and by 10% during autumn (Figure 8). This indicates a limited influence of sea-spray OM on the CCN fraction of CN in the North Atlantic MBL even at a higher supersaturation (0.3%).

The CCN-to-CN fraction at 0.1% supersaturation was lower during continental periods than during marine periods. This result is consistent with past findings that higher contributions of combustion-related organic components reduce particle hygroscopicity (Duplissy et al., 2011; Jimenez et al., 2009; Petters & Kreidenweis, 2007; Wu et al., 2013). The campaign-averaged CCN/CN ratios at 0.1% supersaturation were 0.14 (continental) and 0.22 (marine) for winter, 0.1 (continental) and 0.22 (marine) for late spring, 0.23 (continental) and 0.18 (marine) for autumn and 0.20 (continental) and 0.24 (marine) for early spring. The calculations show that the reason for this change in CCN/CN ratio is the higher fraction of organic mass relative to more hygroscopic sulfate and other salts. This effect is also evident in the reduced hygroscopicity of the aerosol during continental periods compared to marine periods, especially for the winter and late spring campaigns.

6. Conclusions

In order to look at the contributions of different chemical components in the North Atlantic, we separated continental and marine periods by four criteria: CN concentrations <1,500 cm^{-3}, 48 hr HYSPLIT back trajectories over ocean, BC < 50 ng/m^3, and radon <500 mBq/m^3. Marine periods accounted for between 30% (late spring) and 51% (winter) of the duration of the cruises. Stricter BC thresholds did not consistently remove periods of time potentially contaminated by ship traffic or other combustion emissions. The BC threshold did not affect apportionment of non-refractory organic and sulfate components except during late spring, for which a stricter BC threshold (25 ng/m^3) resulted in a lack of correlation between non-refractory Org and $SO_4^{=}$ components and BC.

The hydroxyl group OM correlated strongly with sodium concentrations during ambient marine periods and the hydroxyl group OM (normalized by sea salt) in bubbled sea-spray aerosol particles correlated with DOC (normalized by salinity), indicating that hydroxyl group OM was representative of sea-spray OM. Hydroxyl group OM normalized by sea salt was highest during autumn (0.4 ± 0.1) in bubbled aerosol but highest in late spring (0.5 ± 0.3) for ambient marine periods. The largest ambient concentrations for sea-spray OM (approximated by hydroxyl group OM, 0.33 $\mu g/m^3$) are during late spring. Sea-spray (primary) particles provide the largest (>60%) contributions to submicron mass and CCN (33%) when wind speed is high and ocean productivity is low (Quinn et al., 2019; Sanchez et al., 2018). This suggests that the composition of sea-spray aerosol changed in late spring, with hydroxyl group OM contributing 45% of the sum of sea-spray OM and sea salt compared to <20% for other seasons, but the difference was not statistically significant likely due to the limited number of filter samples during clean marine periods for each campaign.

Secondary OM and sulfate components contributed between 18% (winter) and 60% (late spring) of submicron aerosol mass, with the remainder consisting of sea-spray OM and sea salt. Non-combustion, likely biogenic, secondary sulfate can contribute 21–86% of submicron mass and up to 66% of CCN number at 0.1% supersaturation by increasing the hygroscopicity and concentration of particles in the 0.1 to 0.2 μm diameter range during ambient marine periods. Ship and continental sources contribute the remaining 14–79% of submicron sulfate and 12–53% of submicron OM components, even during clean periods. The seasonal concentrations calculated for marine periods after excluding the influence of combustion sources illustrates the substantial role of secondary marine non-combustion sources for the non-refractory sulfate and organic

components in the MBL during plankton blooms. The combustion source contributions to ambient marine periods illustrate the pervasiveness of contributions from ship and continental sources to open ocean conditions in the North Atlantic. In addition, the differences among the campaigns in the degree to which marine and continental periods could be separated into distinct categories (i.e., autumn marine included 79% non-marine sulfate but late spring marine included only 28% non-marine sulfate) may affect the degree to which seasonal cycles of biogenic source contributions could be hidden by compensating seasonal differences in continental source contributions.

The late spring marine season (plankton biomass climax) is characterized by higher CN, submicron mass, and CCN compared to winter and autumn. The higher calculated CCN concentrations for late spring are a result of the higher particle number concentrations and the larger sulfate mass in the accumulation range. This result, previously reported by Sanchez et al. (2018) and Quinn et al. (2019), indicates that contributions of biogenic non-sea-salt sulfate to particles in the accumulation range likely provide the strongest link between seawater biology and aerosol-cloud interactions at 0.1% supersaturation. For early spring, the CCN/CN fraction for particles in the 0.1–0.2 μm mobility diameter range was higher compared to other seasons for marine periods due to the higher hygroscopicity of the increased fraction of biogenic non-refractory sulfate.

For supersaturations of 0.1–0.3% all particles larger than 0.2 μm in diameter were CCN, assuming the measured chemical composition was internally mixed and that the OM had a κ of 0.1. At 0.3% supersaturation, sea-spray OM reduced CCN number concentrations in the MBL by <5% during winter and late spring and by 13% during autumn when sea-spray OM was assumed to reduce κ by replacing some of the more hygroscopic sulfate. Continental periods had particle number concentrations that were a factor of 3 higher than marine periods, but the submicron particles were (i) less hygroscopic because of the higher contribution from non-refractory organic mass and (ii) likely externally mixed because of the lower measured than calculated CCN when assuming an internal mixture. The combination of the higher CN and lower hygroscopicity resulted in a smaller increase in CCN concentration of only a factor of 1.8, meaning that CCN are not as sensitive as CN to transported continental sources (Martin et al., 2017).

Data Availability Statement

All NAAMES data are available at https://naames.larc.nasa.gov. Scripps measurements are available at https://library.ucsd.edu/dc/collection/bb34508432. Shipboard measurements are archived at https://sea-bass.gsfc.nasa.gov/.

Acknowledgments

The authors would like to thank the dedicated officers and crew of the RV *Atlantis*. The authors also would like to acknowledge Raghu Betha, Derek Price, Derek Coffman, and Lucia Upchurch for their contributions to collecting and reducing data. This work was funded by NASA grant NNX15AE66G and NSF OCE-1537943. This is PMEL contribution number 5070.

References

Aiken, A. C., Salcedo, D., Cubison, M. J., Huffman, J. A., DeCarlo, P. F., Ulbrich, I. M., et al. (2009). Mexico City aerosol analysis during MILAGRO using high resolution aerosol mass spectrometry at the urban supersite (T0)—Part 1: Fine particle composition and organic source apportionment. *Atmospheric Chemistry and Physics*, *9*(17), 6633–6653. https://doi.org/10.5194/acp-9-6633-2009

Alfarra, M. R., Prevot, A. S. H., Szidat, S., Sandradewi, J., Weimer, S., Lanz, V. A., et al. (2007). Identification of the mass spectral signature of organic aerosols from wood burning emissions. *Environmental Science and Technology*, *41*(16), 5770–5777. https://doi.org/10.1021/es062289b

Ayers, G. P., Ivey, J. P., & Gillett, R. W. (1991). Coherence between seasonal cycles of dimethyl sulphide, methanesulphonate and sulphate in marine air. *Nature*, *349*(6308), 404–406. https://doi.org/10.1038/349404a0

Bates, T. S., Calhoun, J. A., & Quinn, P. K. (1992). Variations in the methanesulfonate to sulfate molar ratio in submicrometer marine aerosol particles over the South Pacific Ocean. *Journal of Geophysical Research*, *97*(D9), 9859–9865. https://doi.org/10.1029/92JD00411

Bates, T. S., Quinn, P. K., Coffman, D. J., Johnson, J. E., Upchurch, L., Saliba, G., et al. (2020). Variability in marine plankton ecosystems are not observed in freshly emitted sea spray aerosol over the North Atlantic Ocean. *Geophysical Research Letters*, *47*, e2019GL085938. https://doi.org/10.1029/2019GL085938

Bates, T. S., Quinn, P. K., Frossard, A. A., Russell, L. M., Hakala, J., Petäjä, T., et al. (2012). Measurements of ocean derived aerosol off the coast of California. *Journal of Geophysical Research*, *117*, D00V15. https://doi.org/10.1029/2012JD017588

Bates, T. S., Quinn, P. K., Coffman, D. J., Johnson, J. E., & Middlebrook, A. M. (2005). Dominance of organic aerosols in the marine boundary layer over the Gulf of Maine during NEAQS 2002 and their role in aerosol light scattering. *Journal of Geophysical Research*, *110*, D18202. https://doi.org/10.1029/2005JD005797

Bates, T. S., Coffman, D. J., Covert, D. S., & Quinn, P. K. (2002). Regional marine boundary layer aerosol size distributions in the Indian, Atlantic, and Pacific oceans: A comparison of INDOEX measurements with ACE-1, ACE-2, and Aerosols99. *Journal of Geophysical Research*, *107*(D19), 8026. https://doi.org/10.1029/2001JD001174

Bates, T. S., Quinn, P. K., Coffman, D. J., Covert, D. S., Miller, T. L., Johnson, J. E., et al. (2004). Marine boundary layer dust and pollutant transport associated with the passage of a frontal system over eastern Asia. *Journal of Geophysical Research*, *109*, D19S19. https://doi.org/10.1029/2003JD004094

Beaupré, S. R., Kieber, D. J., Keene, W. C., Long, M. S., Maben, J. R., Lu, X., et al. (2019). Oceanic efflux of ancient marine dissolved organic carbon in primary marine aerosol. *Science Advances*, *5*(10), eaax6535. https://doi.org/10.1126/sciadv.aax6535

Behrenfeld, M. J., Moore, R. H., Hostetler, C. A., Graff, J., Gaube, P., Russell, L. M., et al. (2019). The North Atlantic Aerosol and Marine Ecosystem Study (NAAMES): Science motive and mission overview. *Frontiers in Marine Science*, *6*(November 2015), 1–25. https://doi.org/10.3389/fmars.2019.00122

Berner, A., Lürzer, C., Pohl, F., Preining, O., & Wagner, P. (1979). The size distribution of the urban aerosol in Vienna. *Science of the Total Environment*, *13*(3), 245–261. https://doi.org/10.1016/0048-9697(79)90105-0

Betha, R., Russell, L. M., Chen, C. L., Liu, J., Price, D. J., Sanchez, K. J., et al. (2018). Larger submicron particles for emissions with residential burning in wintertime San Joaquin Valley (Fresno) than for vehicle combustion in summertime South Coast Air Basin (Fontana). *Journal of Geophysical Research: Atmospheres*, *123*, 10–526. https://doi.org/10.1029/2017JD026730

Betha, R., Russell, L. M., Sanchez, K. J., Liu, J., Price, D. J., Lamjiri, M. A., et al. (2017). Lower NO_x but higher particle and black carbon emissions from renewable diesel compared to ultra low sulfur diesel in at-sea operations of a research vessel. *Aerosol Science and Technology*, *51*(2), 123–134. https://doi.org/10.1080/02786826.2016.1238034

Cabada, J. C., Pandis, S. N., Subramanian, R., Robinson, A. L., Polidori, A., & Turpin, B. (2004). Estimating the secondary organic aerosol contribution to PM2.5 using the EC tracer method special issue of aerosol science and technology on findings from the fine particulate matter supersites program. *Aerosol Science and Technology*, *38*(sup1), 140–155. https://doi.org/10.1080/02786820390229084

Cachier, H., Buat-Ménard, P., Fontugne, M., & Chesselet, R. (1986). Long-range transport of continentally-derived particulate carbon in the marine atmosphere: Evidence from stable carbon isotope studies. *Tellus B: Chemical and Physical Meteorology*, *38B*(3–4), 161–177. https://doi.org/10.1111/j.1600-0889.1986.tb00184.x

Carlson, C. A., Hansell, D. A., Nelson, N. B., Siegel, D. A., Smethie, W. M., Khatiwala, S., et al. (2010). Dissolved organic carbon export and subsequent remineralization in the mesopelagic and bathypelagic realms of the North Atlantic basin. *Deep-Sea Research Part II: Topical Studies in Oceanography*, *57*(16), 1433–1445. https://doi.org/10.1016/j.dsr2.2010.02.013

Cavalli, F., Facchini, M. C., Decesari, S., Mircea, M., Emblico, L., Fuzzi, S., et al. (2004). Advances in characterization of size-resolved organic matter in marine aerosol over the North Atlantic. *Journal of Geophysical Research*, *109*, D24215. https://doi.org/10.1029/2004JD005137

Ceburnis, D., Garbaras, A., Szidat, S., Rinaldi, M., Fahrni, S., Perron, N., et al. (2011). Quantification of the carbonaceous matter origin in submicron marine aerosol by ^{13}C and ^{14}C isotope analysis. *Atmospheric Chemistry and Physics*, *11*(16), 8593–8606. https://doi.org/10.5194/acp-11-8593-2011

Chen, Q., Sherwen, T., Evans, M., & Alexander, B. (2018). DMS oxidation and sulfur aerosol formation in the marine troposphere: A focus on reactive halogen and multiphase chemistry. *Atmospheric Chemistry and Physics*, *18*(18), 13,617–13,637. https://doi.org/10.5194/acp-18-13617-2018

Choi, Y., Rhee, T. S., Collett, J. L. Jr., Park, T., Park, S. M., Seo, B. K., et al. (2017). Aerosol concentrations and composition in the North Pacific marine boundary layer. *Atmospheric Environment*, *171*, 165–172. https://doi.org/10.1016/j.atmosenv.2017.09.047

Cubison, M. J., Ortega, A. M., Hayes, P. L., Farmer, D. K., Day, D., Lechner, M. J., et al. (2011). Effects of aging on organic aerosol from open biomass burning smoke in aircraft and laboratory studies. *Atmospheric Chemistry and Physics*, *11*(23), 12,049–12,064. https://doi.org/10.5194/acp-11-12049-2011

Cui, T., Green, H. S., Selleck, P. W., Zhang, Z., O'Brien, R. E., Gold, A., et al. (2019). Chemical characterization of isoprene- and monoterpene-derived secondary organic aerosol tracers in remote marine aerosols over a quarter century. *ACS Earth and Space Chemistry*, *3*(6), 935–946. https://doi.org/10.1021/acsearthspacechem.9b00061

Decesari, S., Finessi, E., Rinaldi, M., Paglione, M., Fuzzi, S., Stephanou, E. G., et al. (2011). Primary and secondary marine organic aerosols over the North Atlantic Ocean during the MAP experiment. *Journal of Geophysical Research*, *116*, D22210. https://doi.org/10.1029/2011JD016204

Devore, J. L., & Berk, K. N. (2012). *Modern mathematical statistics with applications*. New York: Springer.

Duplissy, J., DeCarlo, P. F., Dommen, J., Alfarra, M. R., Metzger, A., Barmpadimos, I., et al. (2011). Relating hygroscopicity and composition of organic aerosol particulate matter. *Atmospheric Chemistry and Physics*, *11*(3), 1155–1165. https://doi.org/10.5194/acp-11-1155-2011

Facchini, M. C., Rinaldi, M., Decesari, S., Carbone, C., Finessi, E., Mircea, M., et al. (2008). Primary submicron marine aerosol dominated by insoluble organic colloids and aggregates. *Geophysical Research Letters*, *35*, L17814. https://doi.org/10.1029/2008GL034210

Falkowski, P. G., Kim, Y., Kolber, Z., Wilson, C., Wirick, C., & Cess, R. (1992). Natural versus anthropogenic factors affecting low-level cloud albedo over the North Atlantic. *Science*, *256*(5061), 1311–1313. https://doi.org/10.1126/science.256.5061.1311

Feichter, J., & Leisner, T. (2009). Climate engineering: A critical review of approaches to modify the global energy balance. *European Physical Journal: Special Topics*, *176*(1), 81–92. https://doi.org/10.1140/epjst/e2009-01149-8

Frossard, A. A., Russell, L. M., Burrows, S. M., Elliott, S. M., Bates, T. S., & Quinn, P. K. (2014). Sources and composition of submicron organic mass in marine aerosol particles. *Journal of Geophysical Research: Atmospheres*, *119*, 12,977–13,003. https://doi.org/10.1002/2014JD021913

Frossard, A. A., Russell, L. M., Massoli, P., Bates, T. S., & Quinn, P. K. (2014). Side-by-side comparison of four techniques explains the apparent differences in the organic composition of generated and ambient marine aerosol particles. *Aerosol Science and Technology*, *48*(3), v–x. https://doi.org/10.1080/02786826.2013.879979

Frossard, A. A., Shaw, P. M., Russell, L. M., Kroll, J. H., Canagaratna, M. R., Worsnop, D. R., et al. (2011). Springtime Arctic haze contributions of submicron organic particles from European and Asian combustion sources. *Journal of Geophysical Research*, *116*, D05205. https://doi.org/10.1029/2010JD015178

Fu, P., Kawamura, K., & Miura, K. (2011). Molecular characterization of marine organic aerosols collected during a round-the-world cruise. *Journal of Geophysical Research*, *116*, D13302. https://doi.org/10.1029/2011JD015604

Gilardoni, S., Russell, L. M., Sorooshian, A., Flagan, R. C., Seinfeld, J. H., Bates, T. S., et al. (2007). Regional variation of organic functional groups in aerosol particles on four U.S. east coast platforms during the International Consortium for Atmospheric Research on Transport and Transformation 2004 campaign. *Journal of Geophysical Research*, *112*, D10S27. https://doi.org/10.1029/2006JD007737

Gysel, M., Laborde, M., Olfert, J. S., Subramanian, R., & Gröhn, A. J. (2011). Effective density of Aquadag and fullerene soot black carbon reference materials used for SP2 calibration. *Atmospheric Measurement Techniques*, *4*(12), 2851–2858. https://doi.org/10.5194/amt-4-2851-2011

Harward, C. N., McClenny, W. A., Hoell, J. M., Williams, J. A., & Williams, B. S. (1982). Ambient ammonia measurements in coastal southeastern Virginia. *Atmospheric Environment*, *16*(10), 2497–2500. https://doi.org/10.1016/0004-6981(82)90140-8

Hawkins, L. N., Russell, L. M., Covert, D. S., Quinn, P. K., & Bates, T. S. (2010). Carboxylic acids, sulfates, and organosulfates in processed continental organic aerosol over the southeast Pacific Ocean during VOCALS-REx 2008. *Journal of Geophysical Research*, *115*, D13201. https://doi.org/10.1029/2009JD013276

Hodshire, A. L., Campuzano-Jost, P., Kodros, J. K., Croft, B., Nault, B. A., Schroder, J. C., et al. (2019). The potential role of methanesulfonic acid (MSA) in aerosol formation and growth and the associated radiative forcings. *Atmospheric Chemistry and Physics*, *19*(5), 3137–3160. https://doi.org/10.5194/acp-19-3137-2019

Hoppel, W. A., Frick, G. M., & Fitzgerald, J. W. (1996). Deducing droplet concentration and supersaturation in marine boundary layer clouds from surface aerosol measurements. *Journal of Geophysical Research*, *101*(D21), 26,553–26,565. https://doi.org/10.1029/96JD02243

Huang, S., Wu, Z., Poulain, L., van Pinxteren, M., Merkel, M., Assmann, D., et al. (2018). Source apportionment of the organic aerosol over the Atlantic Ocean from 53° N to 53° S: Significant contributions from marine emissions and long-range transport. *Atmospheric Chemistry and Physics*, *18*(24), 18,043–18,062. https://doi.org/10.5194/acp-18-18043-2018

Huebert, B. J., Wylie, D. J., Zhuang, L., & Heath, J. A. (1996). Production and loss of methanesulfonate and non-sea salt sulfate in the equatorial Pacific marine boundary layer. *Geophysical Research Letters*, *23*(7), 737–740. https://doi.org/10.1029/96GL00777

Huebert, B. J., Zhuang, L., Howell, S., Noone, K., & Noone, B. (1996). Sulfate, nitrate, methanesulfonate, chloride, ammonium, and sodium measurements from ship, island, and aircraft during the Atlantic stratocumulus transition experiment/marine aerosol gas exchange. *Journal of Geophysical Research*, *101*(D2), 4413–4423. https://doi.org/10.1029/95JD02044

Jefferson, A. (1998). OH photochemistry and methane sulfonic acid formation in the coastal Antarctic boundary layer. *Journal of Geophysical Research*, *103*(D1), 1647–1656. https://doi.org/10.1029/97JD02376

Jickells, T. D., Kelly, S. D., Baker, A. R., Biswas, K., Dennis, P. F., Spokes, L. J., et al. (2003). Isotopic evidence for a marine ammonia source. *Geophysical Research Letters*, *30*(7), 1374. https://doi.org/10.1029/2002GL016728

Jimenez, J. L., Canagaratna, M. R., Donahue, N. M., Prevot, A. S. H., Zhang, Q., Kroll, J. H., et al. (2009). Evolution of organic aerosols in the atmosphere. *Science*, *326*(5959), 1525–1529. https://doi.org/10.1126/science.1180353

Jung, J., Furutani, H., Uematsu, M., & Park, J. (2014). Distributions of atmospheric non-sea-salt sulfate and methanesulfonic acid over the Pacific Ocean between 48°N and 55°S during summer. *Atmospheric Environment*, *99*, 374–384. https://doi.org/10.1016/j.atmosenv.2014.10.009

Kanitz, T., Ansmann, A., Engelmann, R., & Althausen, D. (2013). North-south cross sections of the vertical aerosol distribution over the Atlantic Ocean from multiwavelength Raman/polarization lidar during Polarstern cruises. *Journal of Geophysical Research: Atmospheres*, *118*, 2643–2655. https://doi.org/10.1002/jgrd.50273

Kasparian, J., Hassler, C., Ibelings, B., Berti, N., Bigorre, S., Djambazova, V., et al. (2017). Assessing the dynamics of organic aerosols over the North Atlantic Ocean. *Scientific Reports*, *7*(1), 45476. https://doi.org/10.1038/srep45476

Keene, W. C., Long, M. S., Reid, J. S., Frossard, A. A., Kieber, D. J., Maben, J. R., et al. (2017). Factors that modulate properties of primary marine aerosol generated from ambient seawater on ships at sea. *Journal of Geophysical Research: Atmospheres*, *122*, 11,961–11,990. https://doi.org/10.1002/2017JD026872

Kieber, D. J., Keene, W. C., Frossard, A. A., Long, M. S., Maben, J. R., Russell, L. M., et al. (2016). Coupled ocean-atmosphere loss of marine refractory dissolved organic carbon. *Geophysical Research Letters*, *43*, 2765–2772. https://doi.org/10.1002/2016GL068273

Köllner, F., Schneider, J., Willis, M. D., Klimach, T., Helleis, F., Bozem, H., et al. (2017). Particulate trimethylamine in the summertime Canadian high Arctic lower troposphere. *Atmospheric Chemistry and Physics*, *17*(22), 13,747–13,766. https://doi.org/10.5194/acp-17-13747-2017

Lewis, E. R., & Schwartz, S. E. (2004). Sea salt aerosol production: Mechanisms, methods, measurements and models—A critical review. In *Geophysical Monograph Series*. https://doi.org/10.1029/152GM01

Lim, H. J., Turpin, B. J., Russell, L. M., & Bates, T. S. (2003). Organic and elemental carbon measurements during ACE-Asia suggest a longer atmospheric lifetime for elemental carbon. *Environmental Science and Technology*, *37*(14), 3055–3061. https://doi.org/10.1021/es020988s

Lim, H. J., & Turpin, B. J. (2002). Origins of primary and secondary organic aerosol in Atlanta: Results of time-resolved measurements during the Atlanta Supersite Experiment. *Environmental Science and Technology*, *36*(21), 4489–4496. https://doi.org/10.1021/es0206487

Lin, C. T., Baker, A. R., Jickells, T. D., Kelly, S., & Lesworth, T. (2012). An assessment of the significance of sulphate sources over the Atlantic Ocean based on sulphur isotope data. *Atmospheric Environment*, *62*, 615–621. https://doi.org/10.1016/j.atmosenv.2012.08.052

Liu, J., Dedrick, J., Russell, L. M., Senum, G. I., Uin, J., Kuang, C., et al. (2018). High summertime aerosol organic functional group concentrations from marine and seabird sources at Ross Island, Antarctica, during AWARE. *Atmospheric Chemistry and Physics*, *18*(12), 8571–8587. https://doi.org/10.5194/acp-18-8571-2018

Maria, S. F., Russell, L. M., Turpin, B. J., Porcja, R. J., Campos, T. L., Weber, R. J., & Huebert, B. J. (2003). Source signatures of carbon monoxide and organic functional groups in Asian Pacific Regional Aerosol Characterization Experiment (ACE-Asia) submicron aerosol types. *Journal of Geophysical Research*, *108*(D23), 8637. https://doi.org/10.1029/2003JD003703

Martin, A. C., Cornwell, G. C., Atwood, S. A., Moore, K. A., Rothfuss, N. E., Taylor, H., et al. (2017). Transport of pollution to a remote coastal site during gap flow from California's interior: Impacts on aerosol composition, clouds, and radiative balance. *Atmospheric Chemistry and Physics*, *17*(2), 1491–1509. https://doi.org/10.5194/acp-17-1491-2017

Martin, G. M., Johnson, D. W., & Spice, A. (1994). The measurement and parameterization of effective radius of droplets in warm stratocumulus clouds. *Journal of the Atmospheric Sciences*, *51*(13), 1823–1842. https://doi.org/10.1175/1520-0469(1994)051<1823:tmapoe>2.0.co;2

Matsumoto, K., Uyama, Y., Hayano, T., & Uematsu, M. (2004). Transport and chemical transformation of anthropogenic and mineral aerosol in the marine boundary layer over the western North Pacific Ocean. *Journal of Geophysical Research*, *109*, D21206. https://doi.org/10.1029/2004JD004696

McGovern, F. M., Raes, F., Van Dingenen, R., & Maring, H. (1999). Anthropogenic influences on the chemical and physical properties of aerosols in the Atlantic subtropical region during July 1994 and July 1995. *Journal of Geophysical Research*, *104*(D12), 14,309–14,319. https://doi.org/10.1029/1999JD900131

Meskhidze, N., & Nenes, A. (2006). Phytoplankton and cloudiness in the southern ocean. *Science*, *314*(5804), 1419–1423. https://doi.org/10.1126/science.1131779

Miyazaki, Y., Kawamura, K., Jung, J., Furutani, H., & Uematsu, M. (2011). Latitudinal distributions of organic nitrogen and organic carbon in marine aerosols over the western North Pacific. *Atmospheric Chemistry and Physics*, *11*(7), 3037–3049. https://doi.org/10.5194/acp-11-3037-2011

Mochida, M., Nishita-Hara, C., Furutani, H., Miyazaki, Y., Jung, J., Kawamura, K., & Uematsu, M. (2011). Hygroscopicity and cloud condensation nucleus activity of marine aerosol particles over the western North Pacific. *Journal of Geophysical Research*, *116*, D06204. https://doi.org/10.1029/2010JD014759

Modini, R. L., Frossard, A. A., Ahlm, L., Russell, L. M., Corrigan, C. E., Roberts, G. C., et al. (2015). Primary marine aerosol-cloud interactions off the coast of California. *Journal of Geophysical Research: Atmospheres*, *120*, 4282–4303. https://doi.org/10.1002/2014JD022963

Moldanová, J., Fridell, E., Popovicheva, O., Demirdjian, B., Tishkova, V., Faccinetto, A., & Focsa, C. (2009). Characterisation of particulate matter and gaseous emissions from a large ship diesel engine. *Atmospheric Environment*, *43*(16), 2632–2641. https://doi.org/10.1016/j.atmosenv.2009.02.008

Moore, R. H., Bahreini, R., Brock, C. A., Froyd, K. D., Cozic, J., Holloway, J. S., et al. (2011). Hygroscopicity and composition of Alaskan Arctic CCN during April 2008. *Atmospheric Chemistry and Physics*, *11*(22), 11,807–11,825. https://doi.org/10.5194/acp-11-11807-2011

Moore, R. H., Cerully, K., Bahreini, R., Brock, C. A., Middlebrook, A. M., & Nenes, A. (2012). Hygroscopicity and composition of California CCN during summer 2010. *Journal of Geophysical Research*, *117*, D00V12. https://doi.org/10.1029/2011JD017352

Moteki, N., & Kondo, Y. (2010). Dependence of laser-induced incandescence on physical properties of black carbon aerosols: Measurements and theoretical interpretation. *Aerosol Science and Technology*, *44*(8), 663–675. https://doi.org/10.1080/02786826.2010.484450

Mukai, H., Yokouchi, Y., & Suzuki, M. (1995). Seasonal variation of methanesulfonic acid in the atmosphere over the Oki islands in the sea of Japan. *Atmospheric Environment*, *29*(14), 1637–1648. https://doi.org/10.1016/1352-2310(95)00057-6

Murphy, D. M., Anderson, J. R., Quinn, P. K., McInnes, L. M., Brechtel, F. J., Kreidenweis, S. M., et al. (1998). Influence of sea-salt on aerosol radiative properties in the Southern Ocean marine boundary layer. *Nature*, *392*(6671), 62–65. https://doi.org/10.1038/32138

O'Dowd, C., Ceburnis, D., Ovadnevaite, J., Vaishya, A., Rinaldi, M., & Facchini, M. C. (2014). Do anthropogenic, continental or coastal aerosol sources impact on a marine aerosol signature at Mace Head? *Atmospheric Chemistry and Physics*, *14*(19), 10,687–10,704. https://doi.org/10.5194/acp-14-10687-2014

O'dowd, C., Ceburnis, D., Ovadnevaite, j., Bialek, j., Stengel, D. B., & Zacharias, M., et al. (2015). Connecting marine productivity to sea-spray via nanoscale biological processes: Phytoplankton Dance or Death Disco? *Scientific Reports*, *5*(1), 14883. https://doi.org/10.1038/srep14883

O'Dowd, C. D., Facchini, M. C., Cavalli, F., Ceburnis, D., Mircea, M., Decesari, S., et al. (2004). Biogenically driven organic contribution to marine aerosol. *Nature*, *431*(7009), 676–680. https://doi.org/10.1038/nature02959

Ovadnevaite, J., Ceburnis, D., Leinert, S., Dall'Osto, M., Canagaratna, M., O'Doherty, S., et al. (2014). Submicron NE Atlantic marine aerosol chemical composition and abundance: Seasonal trends and air mass categorization. *Journal of Geophysical Research: Atmospheres*, *119*, 11,850–11,863. https://doi.org/10.1002/2013JD021330

Ovadnevaite, J., Ceburnis, D., Martucci, G., Bialek, J., Monahan, C., Rinaldi, M., et al. (2011). Primary marine organic aerosol: A dichotomy of low hygroscopicity and high CCN activity. *Geophysical Research Letters*, *38*, L21806. https://doi.org/10.1029/2011GL048869

Ovadnevaite, J., O'Dowd, C., Dall'Osto, M., Ceburnis, D., Worsnop, D. R., & Berresheim, H. (2011). Detecting high contributions of primary organic matter to marine aerosol: A case study. *Geophysical Research Letters*, *38*, L02807. https://doi.org/10.1029/2010GL046083

Petters, M. D., & Kreidenweis, S. M. (2007). A single parameter representation of hygroscopic growth and cloud condensation nucleus activity. *Atmospheric Chemistry and Physics*, *7*(8), 1961–1971. https://doi.org/10.5194/acp-7-1961-2007

Quinn, P. K., Bates, T. S., Coffman, D. J., & Covert, D. S. (2008). Influence of particle size and chemistry on the cloud nucleating properties of aerosols. *Atmospheric Chemistry and Physics*, *8*(4), 1029–1042. https://doi.org/10.5194/acp-8-1029-2008

Quinn, P. K., Bates, T. S., Coffman, D. J., Upchurch, L., Johnson, J. E., Moore, R., et al. (2019). Seasonal variations in western North Atlantic remote marine aerosol properties. *Journal of Geophysical Research: Atmospheres*, *124*, 14,240–14,261. https://doi.org/10.1029/2019JD031740

Quinn, P. K., Charlson, R. J., & Zoller, W. H. (1987). Ammonia, the dominant base in the remote marine troposphere: A review. *Tellus B: Chemical and Physical Meteorology*, *39B*(5), 413–425. https://doi.org/10.1111/j.1600-0889.1987.tb00203.x

Quinn, P. K., Coffman, D. J., Johnson, J. E., Upchurch, L. M., & Bates, T. S. (2017). Small fraction of marine cloud condensation nuclei made up of sea spray aerosol. *Nature Geoscience*, *10*(9), 674–679. https://doi.org/10.1038/ngeo3003

Quinn, P. K., Coffman, D. J., Kapustin, V. N., Bates, T. S., & Covert, D. S. (1998). Aerosol optical properties in the marine boundary layer during the First Aerosol Characterization Experiment (ACE 1) and the underlying chemical and physical aerosol properties. *Journal of Geophysical Research*, *103*(D13), 16,547–16,563. https://doi.org/10.1029/97JD02345

Quinn, P. K., Bates, T. S., Schulz, K. S., Coffman, D. J., Frossard, A. A., Russell, L. M., et al. (2014). Contribution of sea surface carbon pool to organic matter enrichment in sea spray aerosol. *Nature Geoscience*, *7*(3), 228–232. https://doi.org/10.1038/ngeo2092

Roberts, G., Mauger, G., Hadley, O., & Ramanathan, V. (2006). North American and Asian aerosols over the eastern Pacific Ocean and their role in regulating cloud condensation nuclei. *Journal of Geophysical Research*, *111*, D13205. https://doi.org/10.1029/2005JD006661

Russell, L. M., Hawkins, L. N., Frossard, A. A., Quinn, P. K., & Bates, T. S. (2010). Carbohydrate-like composition of submicron atmospheric particles and their production from ocean bubble bursting. *Proceedings of the National Academy of Sciences*, *107*(15), 6652–6657. https://doi.org/10.1073/pnas.0908905107

Saliba, G., Chen, C. L., Lewis, S., Russell, L. M., Rivellini, L. H., Lee, A. K. Y., et al. (2019). Factors driving the seasonal and hourly variability of sea-spray aerosol number in the North Atlantic. *Proceedings of the National Academy of Sciences*, *116*(41), 20,309–20,314. https://doi.org/10.1073/pnas.1907574116

Saltzman, E. S., Savoie, D. L., Zika, R. G., & Prospero, J. M. (1983). Methane sulfonic acid in the marine atmosphere. *Journal of Geophysical Research*, *88*(C15), 10,897. https://doi.org/10.1029/JC088ic15p10897

Sanchez, K. J., Chen, C. L., Russell, L. M., Betha, R., Liu, J., Price, D. J., et al. (2018). Substantial seasonal contribution of observed biogenic sulfate particles to cloud condensation nuclei. *Scientific Reports*, *8*(1), 3235. https://doi.org/10.1038/s41598-018-21590-9

Savoie, D. L., Prospero, J. M., Arimoto, R., & Duce, R. A. (1994). Non-sea-salt sulfate and methanesulfonate at American Samoa. *Journal of Geophysical Research*, *99*(D2), 3587. https://doi.org/10.1029/93JD03337

Savoie, D. L., Arimoto, R., Keene, W. C., Prospera, J. M., Duce, R. A., & Galloway, J. N. (2002). Marine biogenic and anthropogenic contributions to non-sea-salt sulfate in the marine boundary layer over the North Atlantic Ocean. *Journal of Geophysical Research*, *107*(D18), 4356. https://doi.org/10.1029/2001JD000970

Schill, S. R., Collins, D. B., Lee, C., Morris, H. S., Novak, G. A., Prather, K. A., et al. (2015). The impact of aerosol particle mixing state on the hygroscopicity of sea spray aerosol. *ACS Central Science*, *1*(3), 132–141. https://doi.org/10.1021/acscentsci.5b00174

Sciare, J., Favez, O., Sarda-Estève, R., Oikonomou, K., Cachier, H., & Kazan, V. (2009). Long-term observations of carbonaceous aerosols in the Austral Ocean atmosphere: Evidence of a biogenic marine organic source. *Journal of Geophysical Research*, *114*, D15302. https://doi.org/10.1029/2009JD011998

Seguin, A. M., Norman, A. L., Eaton, S., & Wadleigh, M. (2011). Seasonality in size segregated biogenic, anthropogenic and sea salt sulfate aerosols over the North Atlantic. *Atmospheric Environment*. https://doi.org/10.1016/j.atmosenv.2011.09.033

Seguin, A. M., Norman, A. L., Eaton, S., Wadleigh, M., & Sharma, S. (2010). Elevated biogenic sulphur dioxide concentrations over the North Atlantic. *Atmospheric Environment*. https://doi.org/10.1016/j.atmosenv.2010.01.005

Seinfeld, J. H., & Pandis, S. N. (2006). *Atmospheric chemistry and physics: From air pollution to climate change* (2nd ed.). Chichester: Wiley.

Shang, D., Hu, M., Guo, Q., Zou, Q., Zheng, J., & Guo, S. (2017). Effects of continental anthropogenic sources on organic aerosols in the coastal atmosphere of East China. *Environmental Pollution*, *229*, 350–361. https://doi.org/10.1016/j.envpol.2017.05.015

Shank, L. M., Howell, S., Clarke, A. D., Freitag, S., Brekhovskikh, V., Kapustin, V., et al. (2012). Organic matter and non-refractory aerosol over the remote Southeast Pacific: Oceanic and combustion sources. *Atmospheric Chemistry and Physics*, *12*(1), 557–576. https://doi.org/10.5194/acp-12-557-2012

Simpson, R. M. C., Howell, S. G., Blomquis, B. W., Clarke, A. D., & Huebert, B. J. (2014). Dimethyl sulfide: Less important than long-range transport as a source of sulfate to the remote tropical pacific marine boundary layer. *Journal of Geophysical Research: Atmospheres*, *119*, 9142–9167. https://doi.org/10.1002/2014JD021643

Snider, J. R., Guibert, S., Brenguier, J. L., & Putaud, J. P. (2003). Aerosol activation in marine stratocumulus clouds: 2. Köhler and parcel theory closure studies. *Journal of Geophysical Research*, *108*(D15), 8629. https://doi.org/10.1029/2002JD002692

Sorooshian, A., Corral, A. F., Braun, R. A., Cairns, B., Crosbie, E., Ferrare, R., et al. (2020). Atmospheric research over the western North Atlantic ocean region and North American East Coast: A review of past work and challenges ahead. *Journal of Geophysical Research: Atmospheres*, *125*, e2019JD031626. https://doi.org/10.1029/2019JD031626

Sorooshian, A., Padró, L. T., Nenes, A., Feingold, G., McComiskey, A., Hersey, S. P., et al. (2009). On the link between ocean biota emissions, aerosol, and maritime clouds: Airborne, ground, and satellite measurements off the coast of California. *Global Biogeochemical Cycles*, *23*, GB4007. https://doi.org/10.1029/2009GB003464

Spracklen, D. V., Arnold, S. R., Sciare, J., Carslaw, K. S., & Pio, C. (2008). Globally significant oceanic source of organic carbon aerosol. *Geophysical Research Letters*, *35*, L12811. https://doi.org/10.1029/2008GL033359

Sullivan, R. C., Petters, M. D., DeMott, P. J., Kreidenweis, S. M., Wex, H., Niedermeier, D., et al. (2010). Irreversible loss of ice nucleation active sites in mineral dust particles caused by sulphuric acid condensation. *Atmospheric Chemistry and Physics*, *10*(23), 11,471–11,487. https://doi.org/10.5194/acp-10-11471-2010

Takahama, S., Johnson, A., Russell, L. M., Takahama, S., & Johnson, A. (2013). Quantification of carboxylic and carbonyl functional groups in organic aerosol infrared absorbance spectra. *Aerosol Science and Technology*, *47*(3), 310–325. https://doi.org/10.1080/02786826.2012.752065

Van Dingenen, R., Raes, F., & Jensen, N. R. (1995). Evidence for anthropogenic impact on number concentration and sulfate content of cloud-processed aerosol particles over the North Atlantic. *Journal of Geophysical Research*, *100*(D10), 21057. https://doi.org/10.1029/95JD02141

Virkkula, A., Teinilä, K., Hillamo, R., Kerminen, V. M., Saarikoski, S., Aurela, M., et al. (2006). Chemical composition of boundary layer aerosol over the Atlantic Ocean and at an Antarctic site. *Atmospheric Chemistry and Physics*, *6*(11), 3407–3421. https://doi.org/10.5194/acp-6-3407-2006

Wex, H., McFiggans, G., Henning, S., & Stratmann, F. (2010). Influence of the external mixing state of atmospheric aerosol on derived CCN number concentrations. *Geophysical Research Letters*, *37*, L10805. https://doi.org/10.1029/2010GL043337

Whittlestone, S., & Zahorowski, W. (1998). Baseline radon detectors for shipboard use: Development and deployment in the First Aerosol Characterization experiment (ACE 1). *Journal of Geophysical Research*, *103*(D13), 16,743–16,751. https://doi.org/10.1029/98JD00687

Wu, Z. J., Poulain, L., Henning, S., Dieckmann, K., Birmili, W., Merkel, M., et al. (2013). Relating particle hygroscopicity and CCN activity to chemical composition during the HCCT-2010 field campaign. *Atmospheric Chemistry and Physics*, *13*(16), 7983–7996. https://doi.org/10.5194/acp-13-7983-2013

Yang, Q., Gustafson, W. I. Jr., Fast, J. D., Wang, H., Easter, R. C., Wang, M., et al. (2012). Impact of natural and anthropogenic aerosols on stratocumulus and precipitation in the Southeast Pacific: A regional modelling study using WRF-Chem. *Atmospheric Chemistry and Physics*, *12*(18), 8777–8796. https://doi.org/10.5194/acp-12-8777-2012

Zhang, Q., Rami Alfarra, M., Worsnop, D. R., Allan, J. D., Coe, H., Canagaratna, M. R., & Jimenez, J. L. (2005). Deconvolution and quantification of hydrocarbon-like and oxygenated organic aerosols based on aerosol mass spectrometry. *Environmental Science and Technology*, *39*(13), 4938–4952. https://doi.org/10.1021/es048568l

Zheng, G., Wang, Y., Aiken, A. C., Gallo, F., Jensen, M. P., Kollias, P., et al. (2018). Marine boundary layer aerosol in the eastern North Atlantic: Seasonal variations and key controlling processes. *Atmospheric Chemistry and Physics*, *18*(23), 17,615–17,635. https://doi.org/10.5194/acp-18-17615-2018

Zorn, S. R., Drewnick, F., Schott, M., Hoffmann, T., & Borrmann, S. (2008). Characterization of the South Atlantic marine boundary layer aerosol using an aerodyne aerosol mass spectrometer. *Atmospheric Chemistry and Physics*, *8*(16), 4711–4728. https://doi.org/10.5194/acp-8-4711-2008